UNCLASSIFIED

AD 210257

Armed Services Technical Information Agency

ARLINGTON HALL STATION
ARLINGTON 12 VIRGINIA

FOR
MICRO-CARD
CONTROL ONLY

1 OF 3

UNCLASSIFIED

AD NO. 210257
ASTIA FILE COPY

FILE COPY

Return to
ASTIA
ARLINGTON HALL STATION
ARLINGTON 12, VIRGINIA
Attn: TISSS

WADC TECHNICAL NOTE 59-32
ASTIA DOCUMENT NR. AD 210257

PRESSURE DISTRIBUTION IN TRANSONIC FLOW OF RIBBON AND GUIDE SURFACE PARACHUTE MODELS

DR. H. G. HEINRICH
DEPARTMENT OF AERONAUTICAL ENGINEERING

MR. J. G. BALLINGER
ROSEMOUNT AERONAUTICAL LABORATORIES

MR. P. E. RYAN
DEPARTMENT OF AERONAUTICAL ENGINEERING

FC

FEBRUARY 1959

THIS REPORT IS NOT TO BE ANNOUNCED OR DISTRIBUTED AUTOMATICALLY IN ACCORDANCE WITH AFR 205-43A, PARAGRAPH 6d

WRIGHT AIR DEVELOPMENT CENTER

WADC TECHNICAL NOTE 59-32
ASTIA DOCUMENT NR. AD 210257

PRESSURE DISTRIBUTION IN TRANSONIC FLOW OF RIBBON AND GUIDE SURFACE PARACHUTE MODELS

DR. H. G. HEINRICH
DEPARTMENT OF AERONAUTICAL ENGINEERING

MR. J. G. BALLINGER
ROSEMOUNT AERONAUTICAL LABORATORIES

MR. P. E. RYAN
DEPARTMENT OF AERONAUTICAL ENGINEERING

FEBRUARY 1959

AERONAUTICAL ACCESSORIES LABORATORY
CONTRACT NR. AF 33(616)-3755
PROJECT NR. 6065
TASK NR. 61510

WRIGHT AIR DEVELOPMENT CENTER
AIR RESEARCH AND DEVELOPMENT COMMAND
UNITED STATES AIR FORCE
WRIGHT-PATTERSON AIR FORCE BASE, OHIO

McGregor & Werner Midwest Corp., Dayton, O.
34-715-100-5-22-59

FOREWORD

This Technical Note was prepared by the Aeronautical Engineering Laboratory of the University of Minnesota. The work was initiated by the Wright Air Development Center, Wright-Patterson Air Force Base, Ohio, and accomplished under Contract AF 33(616)-3755. It was administered by the Parachute Branch of the Aeronautical Accessories Laboratory.

Acknowledgement and appreciation is given to Sandia Corporation, Albuquerque, New Mexico for providing the funds required for the assembly and publication of the data in its present form.

ABSTRACT

The pressure distributions over the canopy of two rigid parachute models were made in a speed range of free stream MACH numbers from .6 to 1.2. Internal and external pressure distributions were conducted on a guide surface and a ribbon model parachute. The results of these data will be used in determining an accurate method of calculating the heat transfer throughout a parachute canopy during descent. Presented are details pertaining to the test methods and equipment used to obtain the experimental data.

PUBLICATION REVIEW

The publication of this report does not constitute approval by the Air Force of the findings or conclusions contained herein. It is published only for the exchange and stimulation of ideas.

FOR THE COMMANDER:

W. P. Shepardson

W. P. SHEPARDSON
Chief, Parachute Branch
Aeronautical Accessories Laboratory

TABLE OF CONTENTS

SYMBOLS USED IN THIS REPORT

P_L = Local static pressure

P_∞ = Free stream static pressure

P_t = Total pressure in the wind tunnel

P_o = Isentropic stagnation temperature

M_∞ = Free stream Mach number

Re = Reynolds number

t = Total temperature in the wind tunnel, °F

γ = Ratio of specific heats = $\frac{C_p}{C_v}$

C_p = Coefficient of pressure defined as:

$$C_p = \frac{P_L - P_\infty}{\frac{\gamma}{2} P_\infty M_\infty^2}$$

I. INTRODUCTION

This report summarizes measurements of pressure distributions over the canopy of two rigid parachute models. This study was originated under Contract No. AF 33(616)-3755, but was discontinued through an executive order on Sept. 6, 1957. Because of related studies pursued by Sandia Corporation, Albuquerque, New Mexico, the evaluation and analysis of already recorded data was requested and sponsored by Sandia Corporation through a purchase request issued on March 3, 1958. The investigation was conducted on a guide surface and a ribbon parachute model with 20% geometric porosity. Both models had a 2.5 inch maximum projected diameter. The tests were made in a speed range of M_∞ = 0.6 to 1.2.

Presented in the body of the report are shadowgraphs, pressure distribution plots and tables for both internal and external pressure distributions. Also presented are summary plots showing the variance of the pressure coefficients for the Mach number range under consideration.

The wind tunnel experiments were conducted in the 12 x 16" transonic wind tunnel of the Rosemount Aeronautical Laboratories.

II. TEST EQUIPMENT

The parachute models were mounted at zero angle of attack and the test range was from M_∞ = 0.6 to M_∞ = 1.25. The Reynolds number range was from 6.99×10^5 to 9.71×10^5 with maximum model diameter of 2.5 inches as the characteristic dimension.

Manuscript released by the author December 1958 for publication as a WADC Technical Note

The models were sting mounted to the balance system. The mounting point of the model to the sting corresponds to the vent hole of a full sized parachute. (See Figs 1, 2, 3 and 4). The ratio of the sting diameter to the maximum diameter was 0.175, the ratio of the sting length to the maximum diameter was 2.95, and for these proportions the sting effects were considered negligible.

The zero angle of attack was measured with reference to the test section center line, however, the data indicated an unsymmetry of less than 0.5 degrees angle of attack. Since both models are bodies of revolution and no reason for truly unsymmetrical pressure distribution can be seen, the obtained data were averaged to symmetry with respect to the model centerlines.

Throughout the wind tunnel tests, shadowgraph pictures were obtained of each experiment. Being free from wall reflected waves, and with sufficiently low dew point temperature, the shadowgraph picture gave a satisfactory indication of the wake and the shock waves.

The guide surface parachute model and the ribbon parachute model gave a blockage effect of 2.56 percent and 0.65 percent, respectively, which is small enough to neglect any wind tunnel corrections for interference effects.

A schematic drawing (Fig 5) shows the manometer board connections. The pressure tap leads are guided internally through the sting and the bundle of tubing leaves the wind tunnel far enough downstream to avoid adverse pressure effects. The free stream Mach number (M_{∞}) was obtained by use of previously calculated calibration charts for

the transonic tunnel considering no interference effects. This arrangement was used for both the guide surface and the ribbon type parachute model.

III. MODEL DETAILS

Three models of each parachute were made. One for shadowgraph pictures, one for the measurement of internal and one for the measurement of external pressure distributions. All models were constructed of 0.037 inch stainless steel and manufactured according to Figs 6, 7, and 8. It should be noted that the guide surface parachute models have an overall diameter of 2.469 inches instead of 2.5 inches. This was caused by the arrangement of a defined radius at the corner of the intersection between the truncated cone and the spherical roof. For simplicity, the model has been referred to as having a 2.5 inch maximum diameter.

Attention is called to damage of the ribbon parachute models shown in Fig 9 and 10, which was caused by high frequency vibration of the models when subjected to transonic flow. In order to prevent this type of damage, crosswisely arranged stiffeners were placed in the inside of the models. These stiffeners were made of two half circles of 0.037 inch stainless steel, with sharpened leading edges. On the basis of a random distribution of the internal pressure taps around the periphery of the model, it was concluded that the stiffeners did not noticably effect the pressure distribution.

Figs 11 and 12 illustrate the locations of pressure taps, the dimensions given in terms of maximum diameter.

IV. PRESSURE DISTRIBUTION

The objective of this project was the determination of the internal and external coefficients of pressure (C_p) for the ribbon and guide surface parachutes for varying Mach numbers.

The coefficient of pressure was defined as:

$$C_p = \frac{\Delta P}{q} = \frac{P_L - P_\infty}{q} = \frac{P_L - P_\infty}{\frac{1}{2}\gamma P_\infty M_\infty^2} = \frac{2}{\gamma M_\infty^2}\left(\frac{P_L}{P_\infty} - 1\right) \quad (1)$$

Where: P_L is the local static pressure

P_∞ is the free stream static pressure

M_∞ is the free stream Mach number

$q = \frac{1}{2}\rho V^2$ is the dynamic pressure

γ is the ratio of specific heats (assumed = 1.40 for temperature range of 72° - 94°F during tests)

In transonic and low supersonic flow, one may expect that inside of a hollow, non-porous or mildly porous object, the local pressure amounts to approximately the isentropic stagnation pressure. In compressible flow the stagnation pressure P_0 can be expressed in terms of the dynamic pressure q by means of the well known relationship.

$$P_0 = P_\infty + q\left(1 + \frac{M_\infty^2}{4} + \frac{M_\infty^4}{40} + \frac{M_\infty^6}{1600} + \cdots +\right) \quad (2)$$

If perfect isentropic stagnation pressure is achieved on the inside of the parachute models, then the pressure coefficient would amount to*

$$C_p = \frac{\Delta P}{q} = 1 + \frac{M_\infty^2}{4} + \frac{M_\infty^4}{40} + \frac{M_\infty^6}{1600} + \cdots + \quad (3)$$

* Liepman, H. W., and Puckett, A.E. "Introduction to Aerodynamics of a Compressible Fluid", Galcit Aeronautical Series, p. 76, John Wiley & Sons, Inc., New York, 1947.

For convenient comparison, the pressure coefficient, $C_{P_{AV}}$, as defined in Eq. 1, measured and averaged over the entire inside of the parachute models, and the value of Eq. 3, which is merely a function of Mach number, is indicated on each schematic presentation of the pressure distribution.

V. EXPERIMENTAL RESULTS

A. Ribbon Type Parachute Model with Twenty Percent Geometric Porosity.

Tests were conducted at the following Mach numbers:

External Pressure	Internal Pressure
M = 0.610	M = 0.612
M = 0.812	M = 0.810
M = 0.904	M = 0.905
M = 0.951	M = 0.956
M = 0.998	M = 1.014
M = 1.061	M = 1.063
M = 1.128	M = 1.115
M = 1.191	M = 1.192

Since these Mach numbers vary only in the third decimal place, average Mach numbers are referred to for simplicity. The average Mach numbers are considered as 0.61, 0.81, 0.90, 0.95, 1.00, 1.12 and 1.19.

Figs 13, 15, 17, 19, 21, 23, 25 and 27 are the shadowgraphs of the flow patterns for the above mentioned Mach numbers.

The combined internal and external pressure coefficients are shown in Figs 14, 16, 18, 20, 22, 24, 26 and 28. Vectors pointing towards the surface of the model indicate positive C_p values, while vectors pointing away indicate negative C_p values.

Fig 29 shows how the pattern of the pressure distribution varies with Mach number .

B. Guide Surface Parachute Model

The pressure distribution for the guide surface parachute model was also determined by eight wind tunnel tests for each model. The tunnel Mach numbers were:

External	Internal
M = 0.615	M = 0.612
M = 0.805	M = 0.801
M = 0.890	M = 0.899
M = 0.930	M = 0.956
M = 1.007	M = 1.015
M = 1.072	M = 1.067
M = 1.130	M = 1.135
M = 1.234	M = 1.230

Again for simplicity and comparison, the experiments were considered to have been performed at Mach numbers of 0.61, 0.80, 0.89, 0.94, 1.01, 1.07, 1.13 and 1.23.

Shadowgraphs showing the flow patterns are presented as Figures 30, 33, 36, 39, 42, 45, 48 and 51 for the above average Mach numbers.

For clarity of presentation, the external and internal pressure distributions are shown on individual figures. As before a vector presentation of the pressure coefficients has been chosen. The external pressure coefficients are shown in Figs 31, 34, 37, 40, 43, 46, 49 and 52 while the internal pressure coefficients are presented in Figs 32, 35, 38, 41, 44, 47, 50 and 53.

Figs 54 and 55 show the external and internal pressure coefficients for the highest and lowest experimental Mach numbers, 1.234 and 0.615 respectively.

VI. ANALYSIS

A. Ribbon Parachute

Shadowgraphs of the flow patterns are shown in Figs 13, 15, 17, 19, 21, 25 and 27. From inspection of the shadowgraphs the following observations may be pointed out.

1. In subsonic flow (Fig 13) a well defined stream of air passes through the slots between the individual ribbons. This picture indicates that this flow is subsonic. Fig 15 shows the same type of flow passing through the slots. By examining the pressure ratio across the parachute canopy one finds that near the parachute skirt, the pressure differential between the inside and outside of the canopy is sufficient to establish sonic flow. However, the shadowgraph does not indicate a significant change compared with the preceding picture.

2. Beginning at Mach number 0.897, Fig 17, the air stream between the ribbons begins to show a diamond pattern which is characteristic of jet flow with sonic speed.

3. The most prominent indications of sonic flow through the slots can be seen in Fig 27 ($M_\infty = 1.194$). Figs 25 and 27 also indicate the pressure of a detached shock wave ahead of the parachute model.

The Fig 17 and 19 prove that supersonic flow may exist in the slots, even though the free stream Mach number is still subsonic, which can be understood in view of the reduced pressure on the outside of the parachute canopy while almost full isentropic stagnation pressure exists inside the parachute canopy.

The individual pressure distribution plots for the ribbon type parachute, Figs 14 and following, show the variation of the external and internal pressure coefficients for each test Mach number. In general, the pressure distribution diagrams show that with increasing Mach numbers the negative value of the external coefficients of pressure decrease while the internal coefficients increase. The net change of pressure distribution, however, represents a decrease in the tendency of inflation of a flexible parachute.

While the pattern of the external pressure distribution changes considerably with Mach number, the internal pressure coefficient assumes in all cases a value approximately equal to ratio of $\frac{\Delta P}{q}$ of compressible flow (see Eq. 3, Page 4).

B. Guide Surface Parachute

Shadowgraph pictures of the flow pattern for the guide surface parachute model are shown in Figs 30 and following. The shadowgraphs are good for purposes of wake visualization, whereas, the expected expansion around the parachute model corner is invisible.

The individual pressure distribution plots are shown in Figs 31 and following. Included in the plots for external pressure distribution is an enlarged scale plot of the pressure distribution about the corner, in which dotted lines indicate an estimate of the pressure coefficient which obviously undergoes strong changes in this region.

The pressure distribution across the roof of the guide surface model does not change appreciably, and also remains nearly constant for any particular free stream Mach number.

Figs 32 and following show that the internal pressure distribution is also nearly constant across the surface of the parachute model and that its amount is nearly equal to the isentropic stagnation pressure.

Fig 54 is a summary plot showing the external pressure coefficient for the extremities of the test range, $M_\infty = 0.615$ and 1.234 respectively. This figure indicates a significant change of the external pressure with Mach number. In combination with Fig 55 it can be seen that the net force, which keeps the parachute inflated, decreases with Mach number.

In Fig 56 there is a continuous presentation of the local external pressure coefficient plotted against the flattened surface of the guide surface parachute. The tap locations correspond to

their actual locations on the surface of the parachute.

Figs 57 and 58 present the same effect in a different manner, and these figures may be of particular interest in studies of the functional behavior of parachutes in transonic and supersonic flow. It appears to be evident that with the approach of the region of compressibility, conventional parachutes will display undesirable characteristics.

The foregoing results have been presented in a quantitative rather than a qualitative manner, which is a consequence of the fact that this study is merely a part of our overall effort to establish the foundation of aerodynamic retardation and this report should be considered as merely advanced information.

APPENDIX

APPENDIX A

LIST OF FIGURES

PAGE

PAGE

APPENDIX B

List of Tables

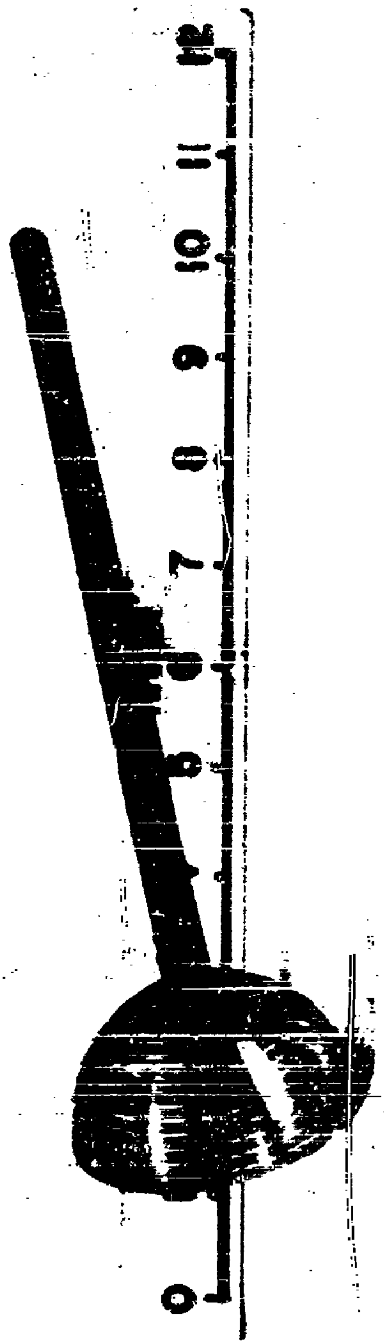

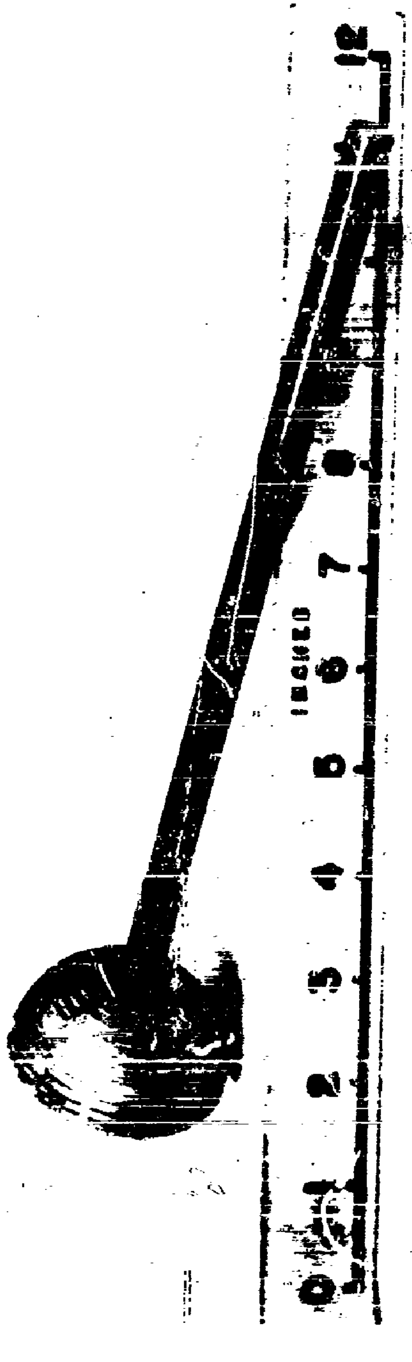

RADC 2- 59-32

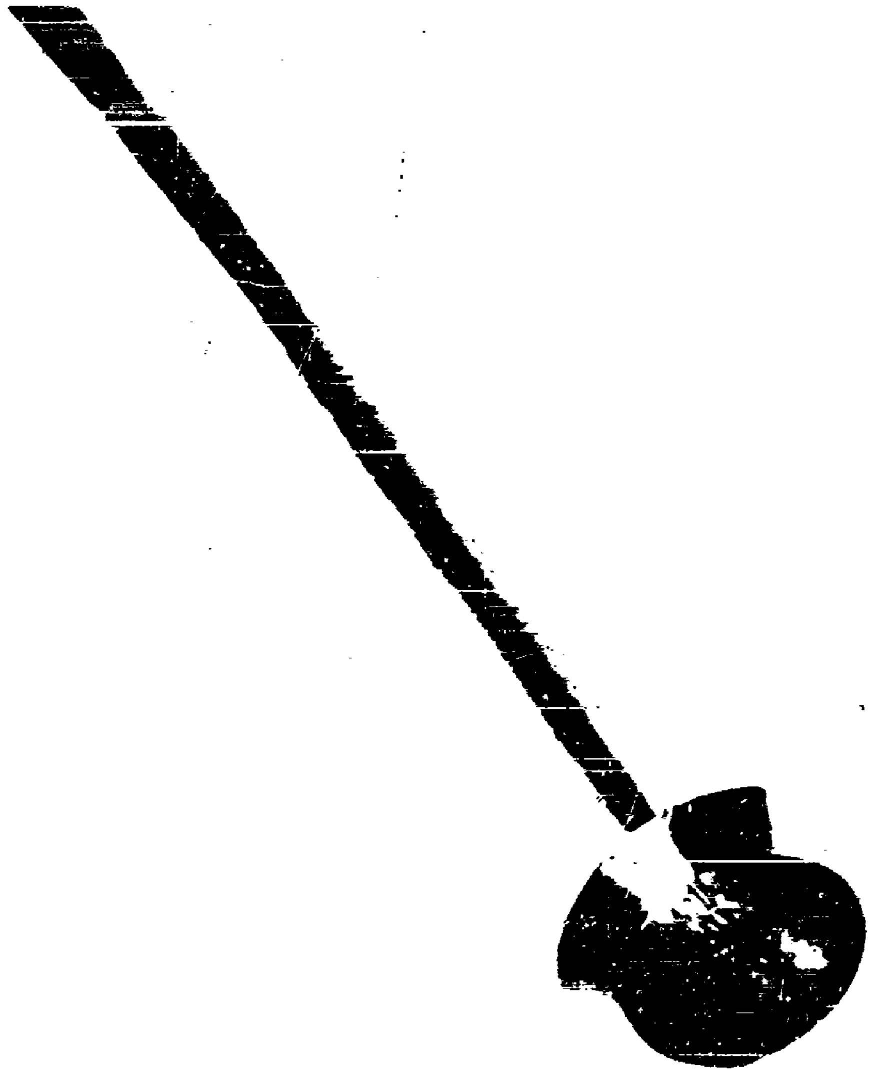

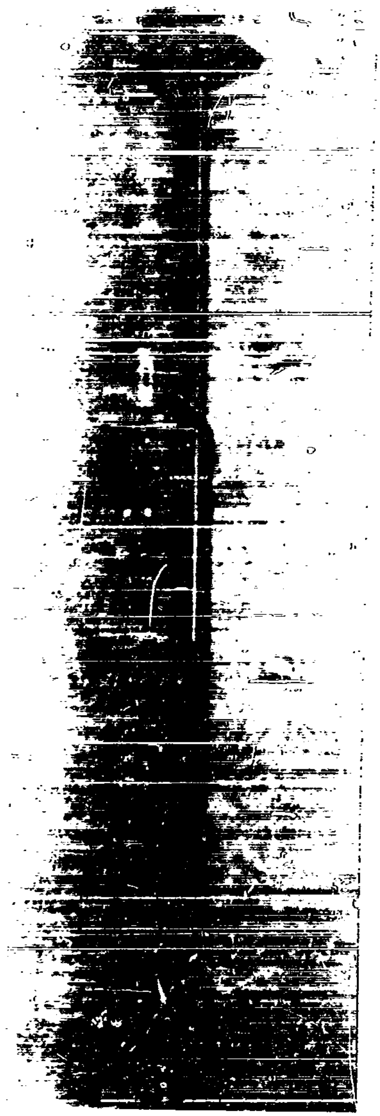

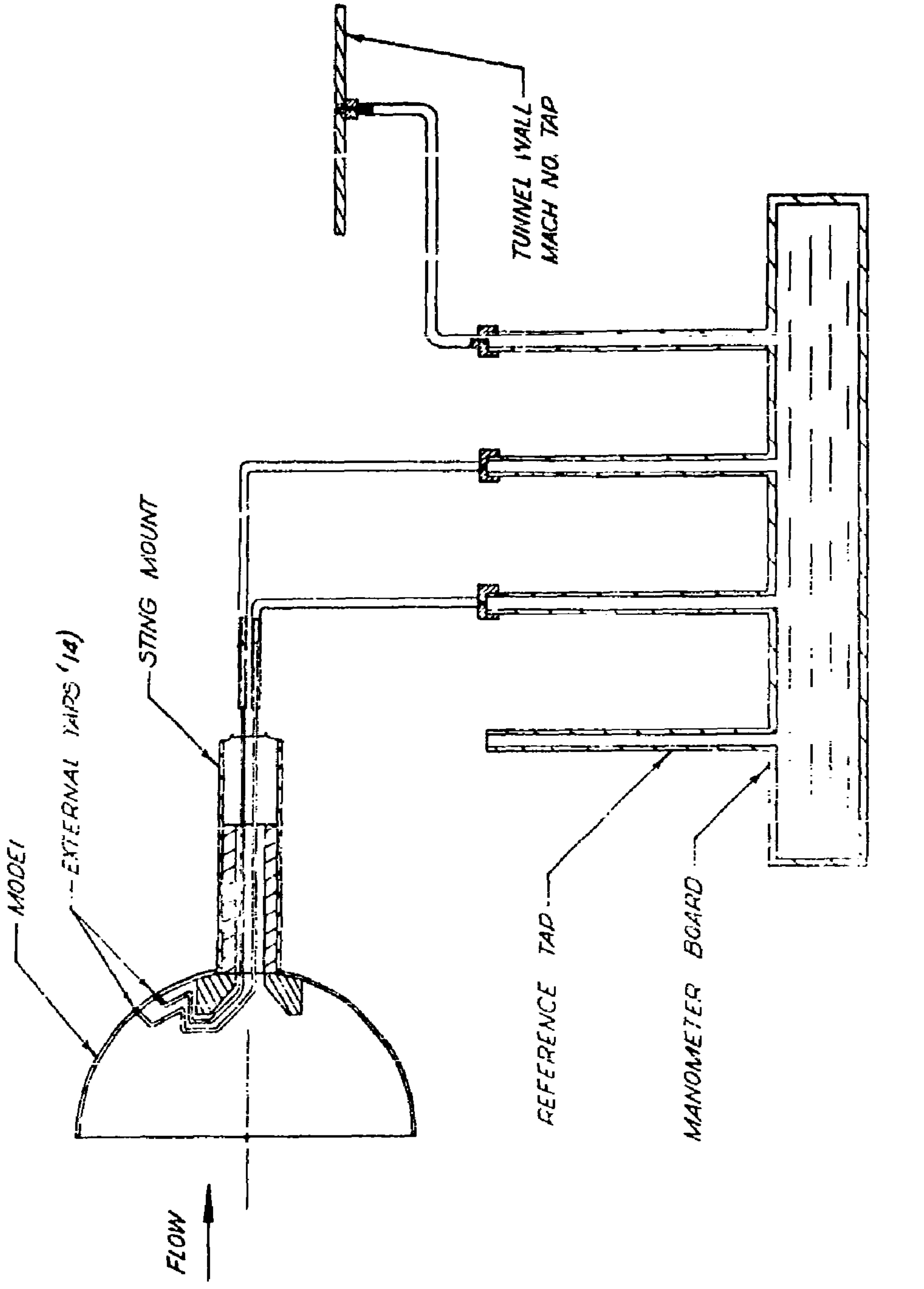

SCHEMATIC OF PRESSURE TAP HOOKUP

FIG. 5

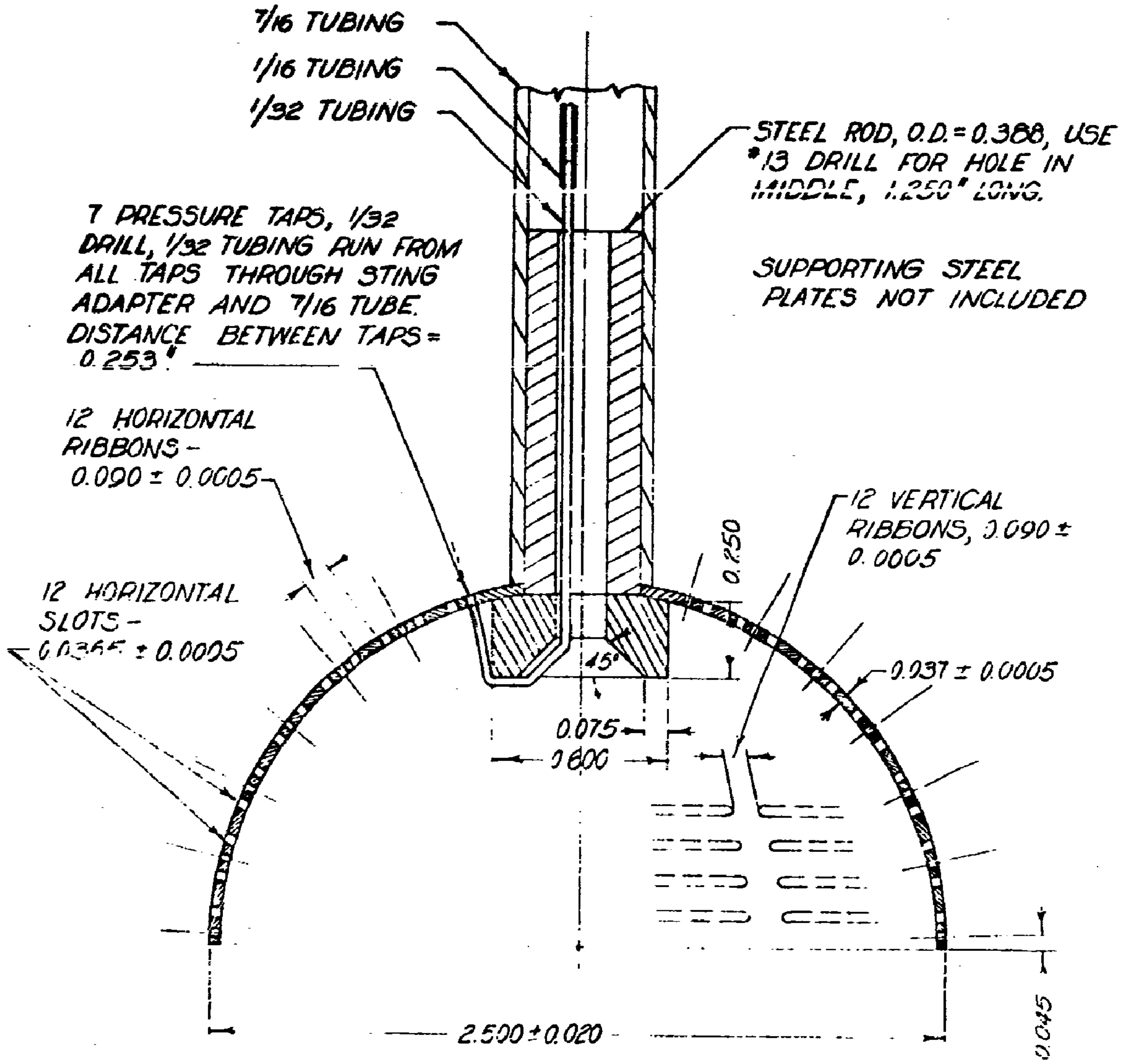

EXTERNAL PRESSURE TAP MODEL

SCALE: 2" = 1"

FIG. 6

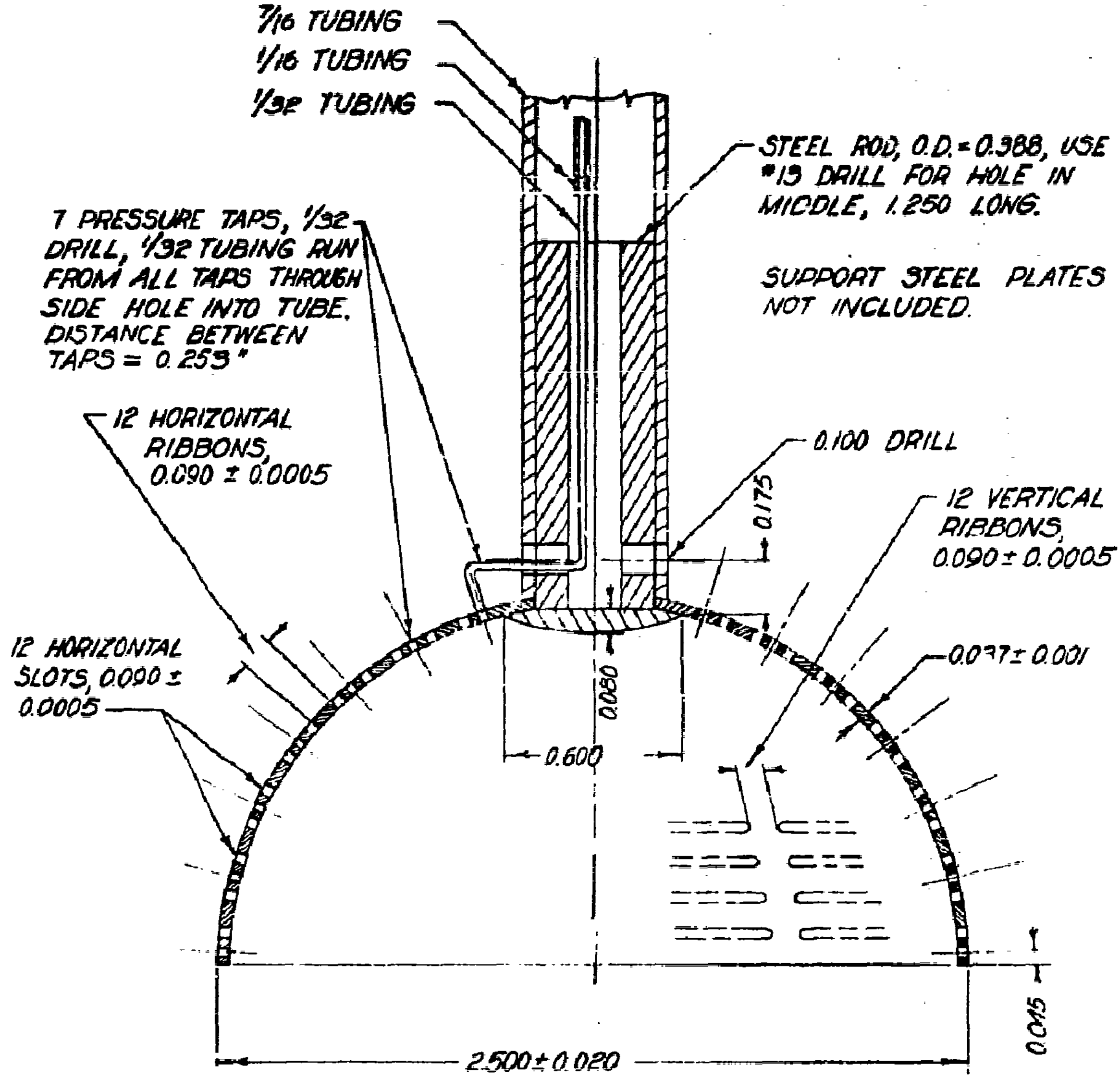

INTERNAL PRESSURE TAP MODEL
SCALE : 2" = 1"

FIG. 7

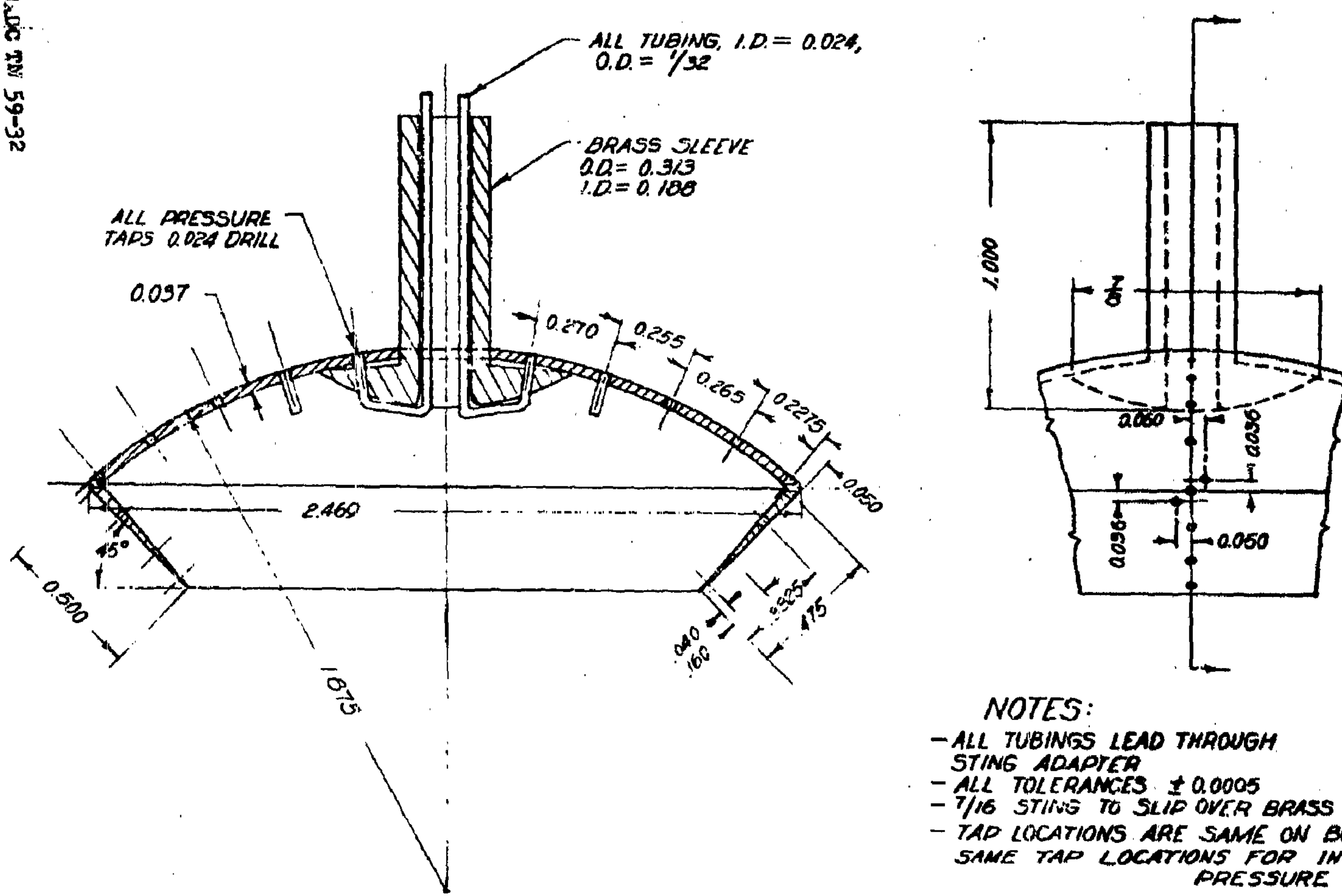

NOTES:
- ALL TUBINGS LEAD THROUGH STING ADAPTER
- ALL TOLERANCES ± 0.0005
- 7/16 STING TO SLIP OVER BRASS SLEEVE
- TAP LOCATIONS ARE SAME ON BOTH SIDE SAME TAP LOCATIONS FOR INTERNAL PRESSURE MODEL

EXTERNAL PRESSURE PARACHUTE MODEL
SCALE: 2" = 1"
FIG 8

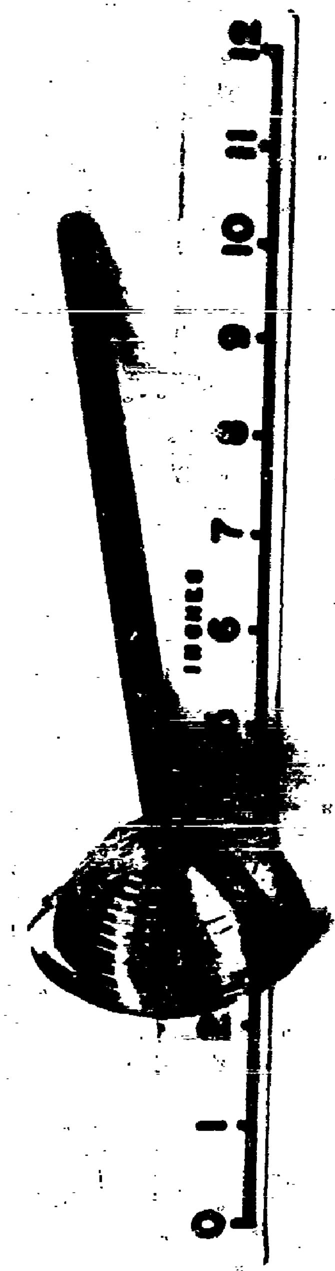

Fig. 8

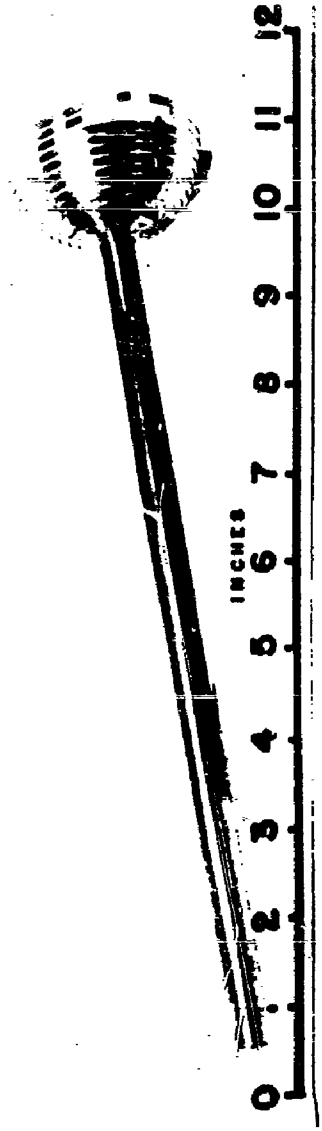
INCHES
0
1
2
3
4
5
6
7
8
9
10
11
12

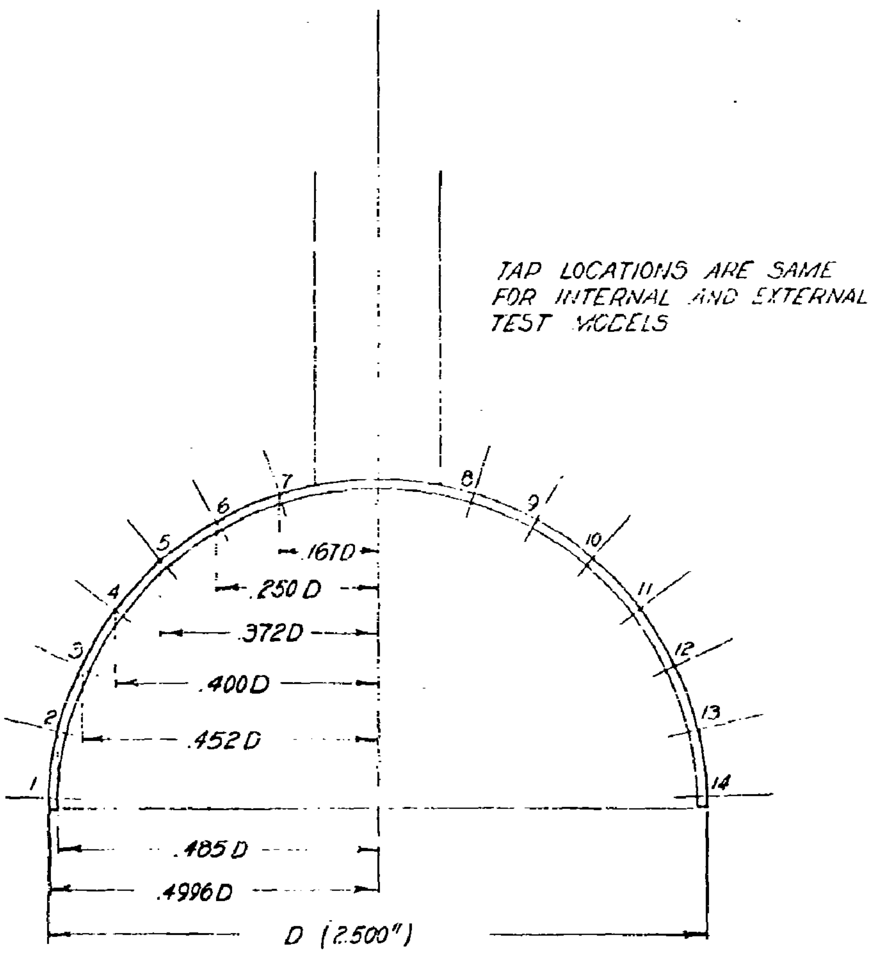

RIBBON PARACHUTE MODEL PRESSURE TAP LOCATIONS IN TERMS OF OVERALL DIAMETER "D."

SCALE: 2" = 1"

FIG. 11

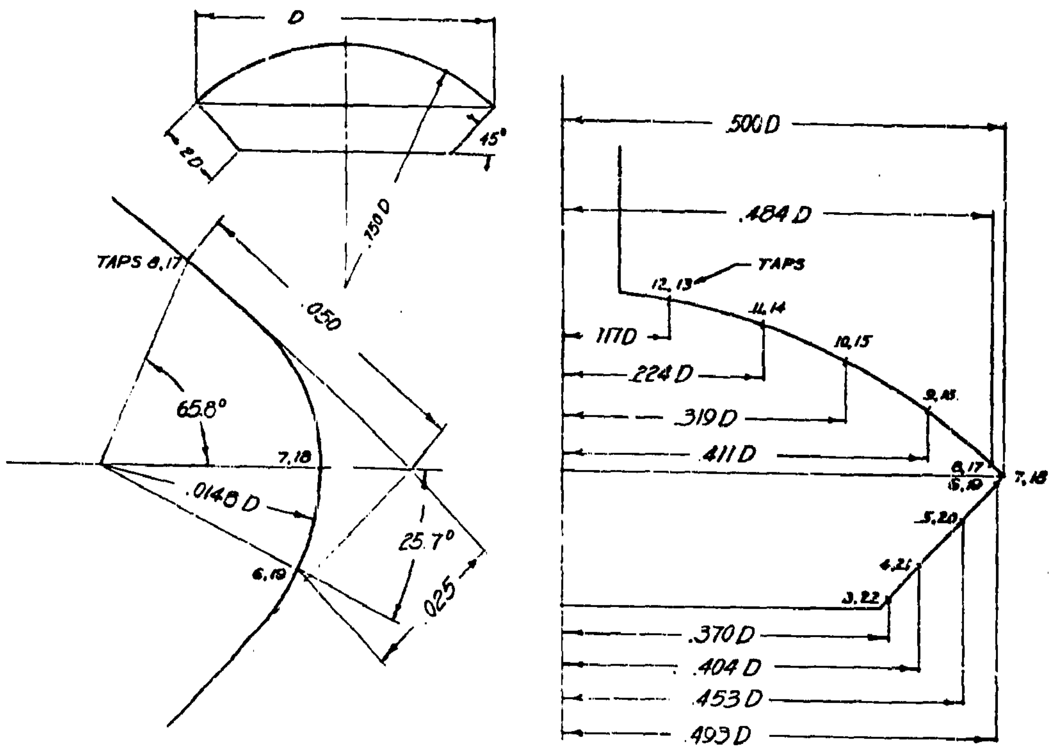

MODEL TIP BLOWUP
SCALE : 50" = 1"

HALF MODEL
SCALE : 3" = 1"

GUIDE SURFACE PARACHUTE TAP LOCATIONS IN TERMS OF OVER L DIA. D
D = 2.500"

FIG. 12

WADC TN 59-32

FIG. 13 Shadowgraph Picture of a Ribbon Parachute Model at Mach Nr. 0.598

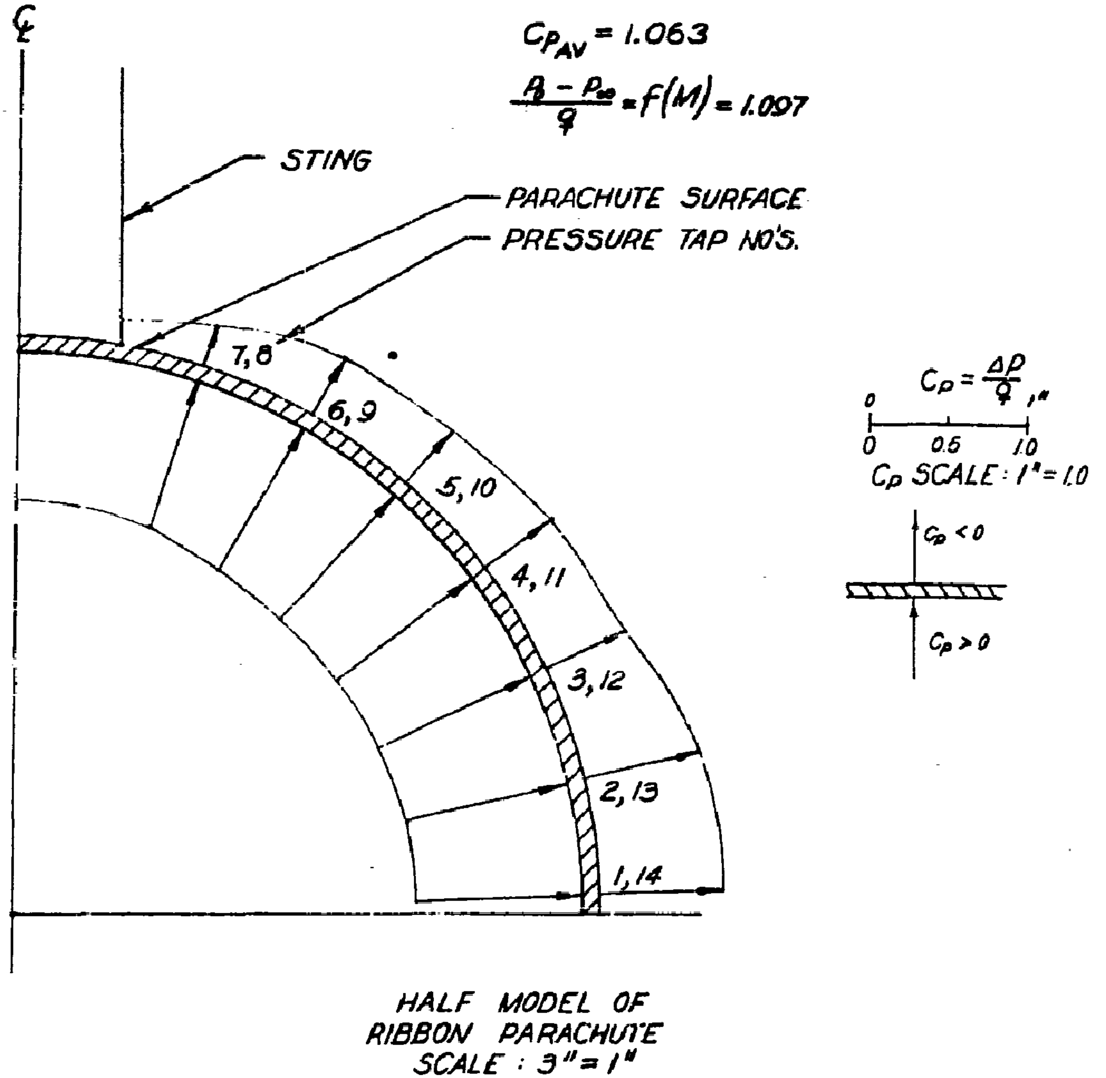

PRESSURE DISTRIBUTION ON A 2.5" RIBBON PARACHUTE $M_\infty \simeq 0.61$

FIG. 14

TABLE NO. 1

RIBBON TYPE PARACHUTE PRESSURE DISTRIBUTION

$M_{\infty_{AV}} =$ 0.61

EXTERNAL PRESSURE TEST			INTERNAL PRESSURE TEST		
$M_\infty =$ 0.610			$M_\infty =$ 0.612		
$P_\infty =$ 11.132 psia		$t =$ 72.9° F	$P_\infty =$ 11.117 psia		$t =$ 71° F
$P_0 =$ 14.309 psia		$Re =$ 7.26 × 10^5	$P_0 =$ 14.312 psia		$Re =$ 7.26 × 10^5
TAP NO.	P_L (psia)	C_p	TAP NO.	P_L (psia)	C_p (+)
1	8.798	-0.805	1	14.25	1.075
2	8.954	-0.751	2	14.21	1.062
3	9.463	-0.575	3	14.24	1.073
4	9.546	-0.547	4	14.27	1.083
5	9.947	-0.408	5	14.25	1.077
6	9.879	-0.432	6	14.28	1.085
7	10.354	-0.268	7	14.04	1.003
8	10.349	-0.270	8	14.02	0.996
9	9.884	-0.430	9	14.18	1.053
10	9.810	-0.456	10	14.28	1.085
11	9.639	-0.515	11	14.26	1.080
12	9.527	-0.553	12	14.27	1.083
13	8.895	-0.771	13	14.21	1.062
14	8.886	-0.775	14	14.23	1.068

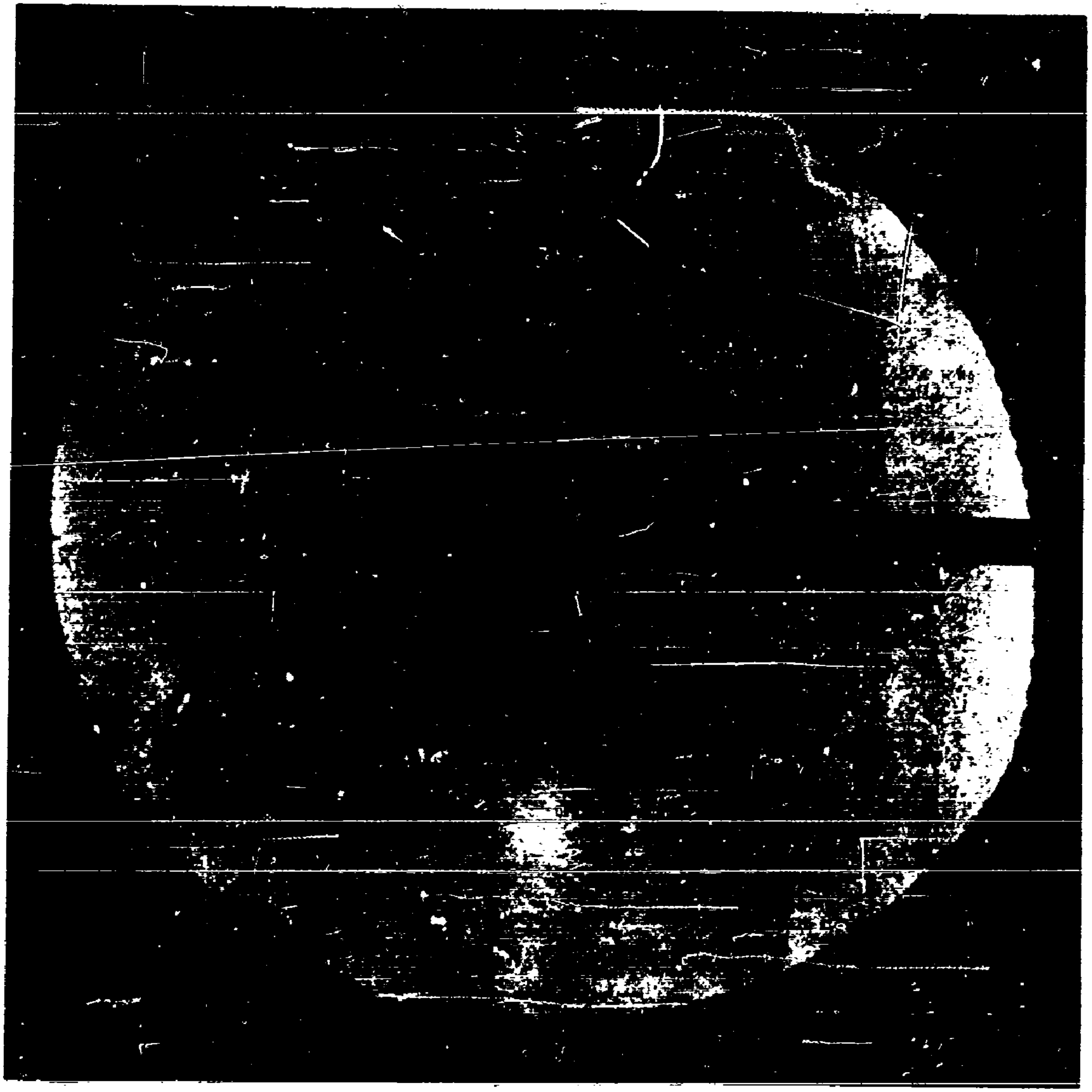

FIG. 15. Shadowgraph Picture of a Ribbon Parachute Model At Mach Nr. 0.805

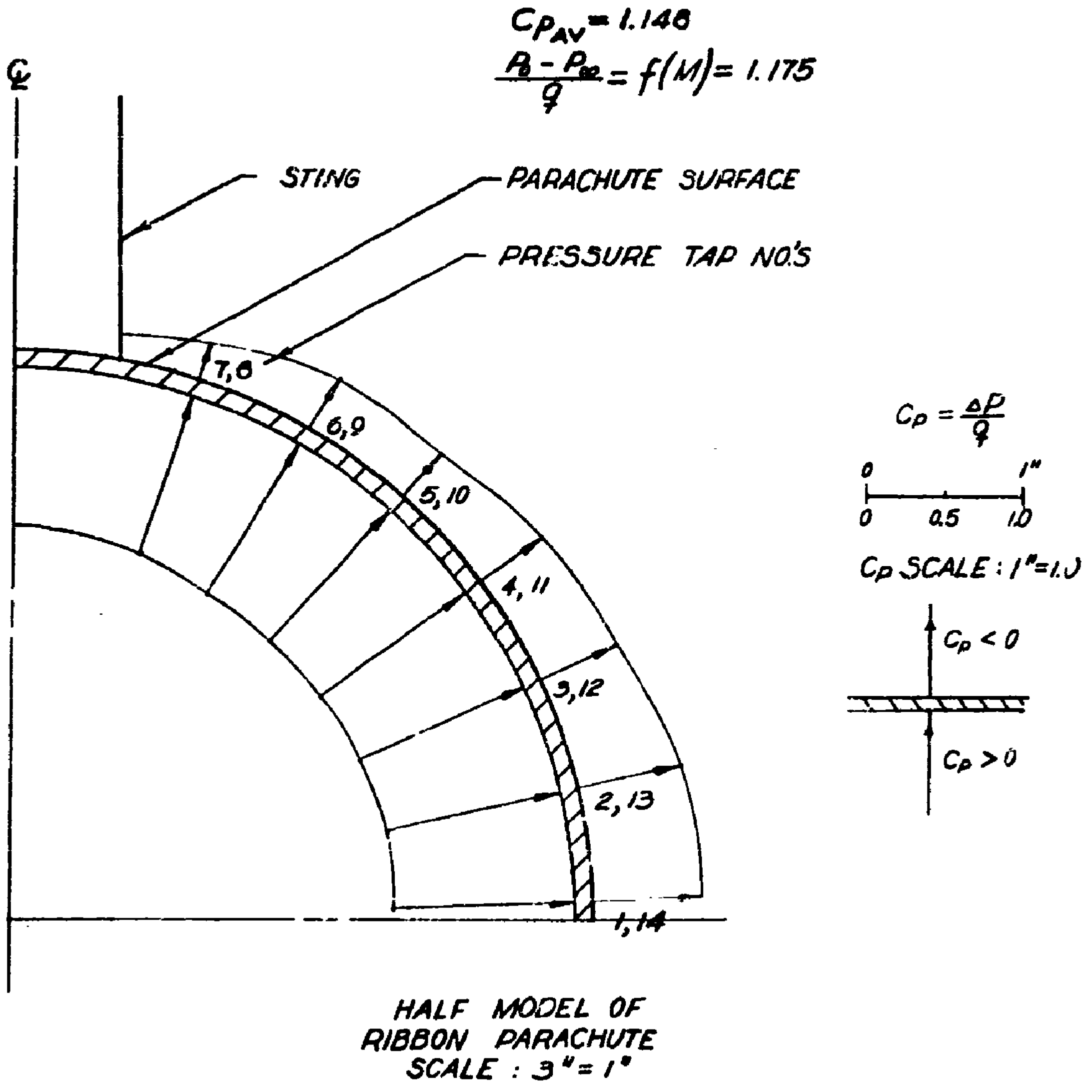

PRESSURE DISTRIBUTION ON A 2.5" RIBBON PARACHUTE $M_\infty = 0.81$

TABLE NO. 2

RIBBON TYPE PARACHUTE PRESSURE DISTRIBUTION

$M_{\infty_{AV}} = 0.81$

EXTERNAL PRESSURE TEST			INTERNAL PRESSURE TEST		
$M_\infty = 0.812$			$M_\infty = 0.810$		
$P_\infty = 9.277$ psia	$t = 72.9^\circ F$		$P_\infty = 9.292$ psia	$t = 71^\circ F$	
$P_0 = 14.369$ psia	$Re = 8.65 \times 10^5$		$P_0 = 14.312$ psia	$Re = 8.69 \times 10^5$	
TAP NO.	P_L (psia)	C_p	TAP NO.	P_L (psia)	C_p (+)
1	6.204	-0.718	1	14.25	1.162
2	6.351	-0.683	2	14.18	1.145
3	6.889	-0.558	3	14.22	1.156
4	7.154	-0.496	4	14.26	1.165
5	7.672	-0.375	5	14.23	1.159
6	7.633	-0.384	6	14.26	1.165
7	8.289	-0.231	7	13.95	1.091
8	8.289	-0.231	8	13.92	1.085
9	7.599	-0.392	9	14.14	1.137
10	9.316	+0.009 *	10	14.27	1.167
11	7.261	-0.471	11	14.25	1.162
12	7.056	-0.519	12	14.26	1.165
13	6.366	-0.680	13	14.18	1.147
14	6.346	-0.685	14	14.23	1.159

* EXTERNAL PRESSURE TEST - TAP NO. 10 BEGAN LEAKING, DISREGARD FOR REMAINDER OF TESTS

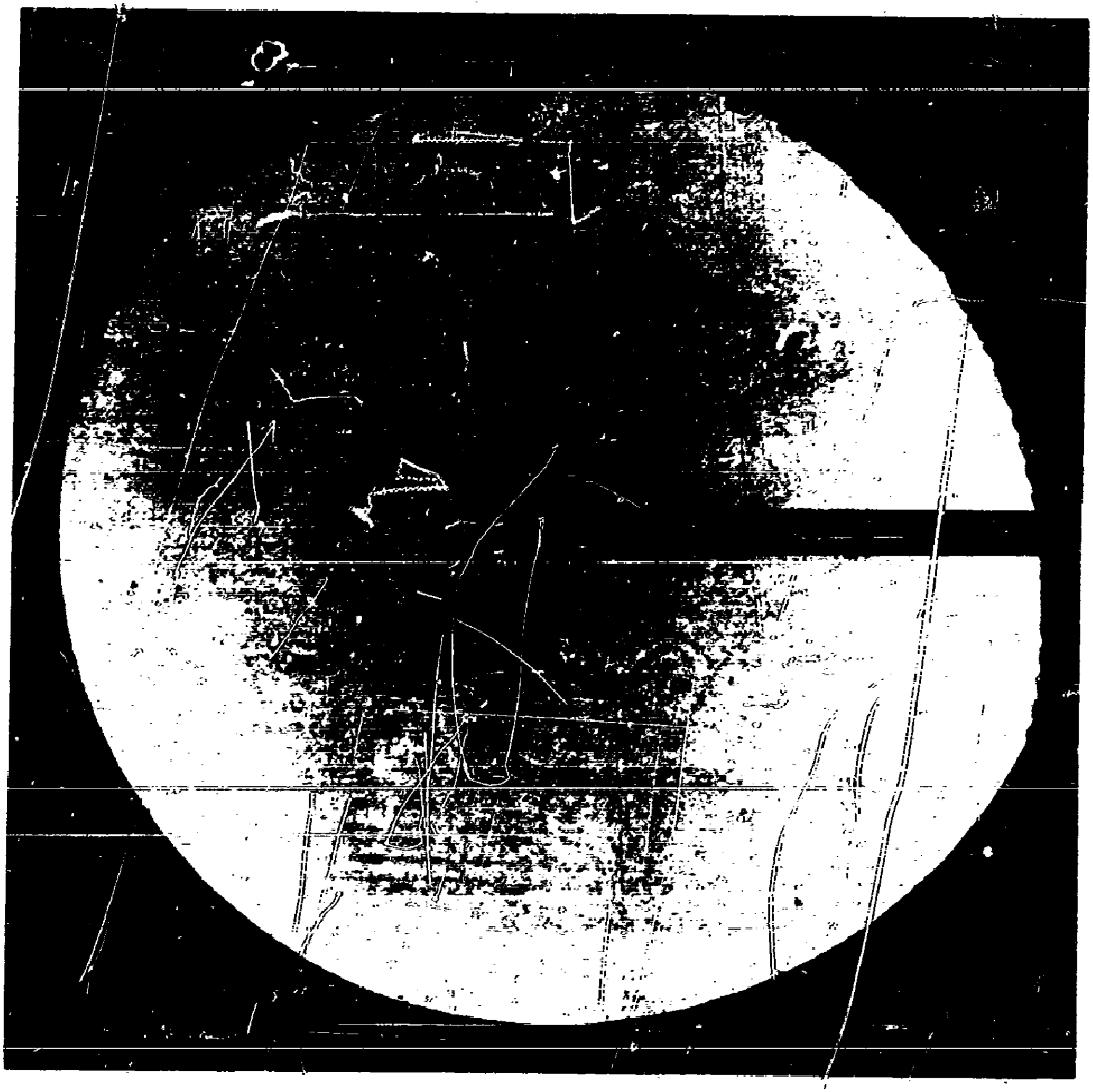

FIG. 17. Shadowgraph Picture of a Ribbon Parachute Model at Mach Nr. 0.897

$Cp_{AV} = 1.199$

$\frac{P_0 - P_\infty}{q} = f(M) = 1.219$

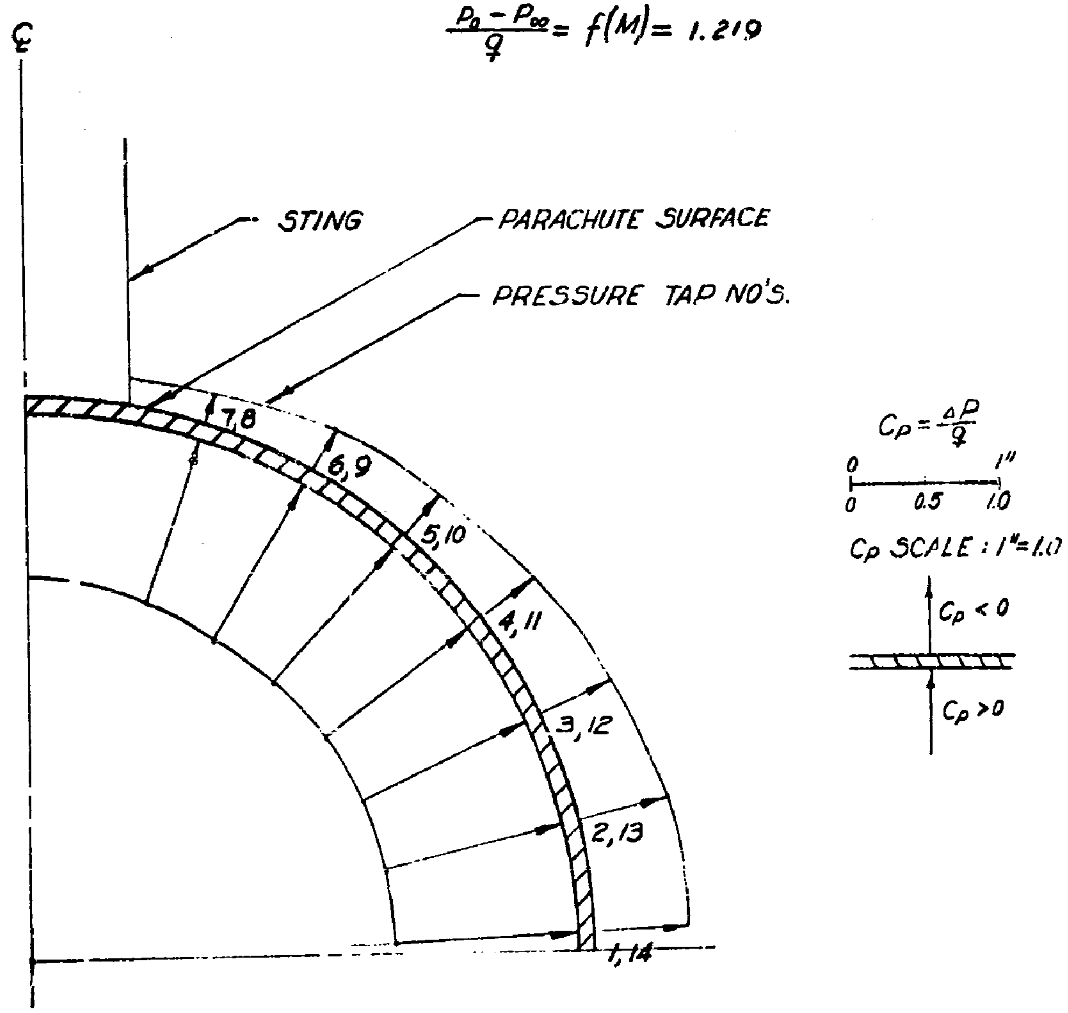

HALF MODEL OF
RIBBON PARACHUTE
SCALE : 3" = 1"

PRESSURE DISTRIBUTION ON A 2.5" RIBBON PARACHUTE $M_\infty \simeq 0.90$

FIG. 18

TABLE NO. 9

RIBBON TYPE PARACHUTE PRESSURE DISTRIBUTION

$M_{\infty} = 0.90$

EXTERNAL PRESSURE TEST			INTERNAL PRESSURE TEST		
$M_{\infty} = 0.904$			$M_{\infty} = 0.905$		
$P_{\infty} = 8.416$ psia	$t = 72.9$ F		$P_{\infty} = 8.406$ psia	$t = 71°$ F	
$P_0 = 14.309$ psia	$Re = 9.11 \times 10^5$		$P_0 = 14.312$ psia	$Re = 9.11 \times 10^5$	
TAP NO.	P_L (psia)	C_p	TAP NO.	P_L (psia)	C_p (+)
1	5.343	-0.638	1	14.24	1.212
2	5.441	-0.619	2	14.17	1.197
3	5.891	-0.526	3	14.22	1.207
4	6.263	-0.448	4	14.26	1.215
5	6.796	-0.338	5	14.23	1.209
6	6.948	-0.307	6	14.23	1.209
7	7.530	-0.186	7	13.93	1.147
8	7.535	-0.185	8	13.90	1.140
9	6.855	-0.326	9	14.14	1.190
10	7.726	-0.145	10	14.27	1.217
11	6.380	-0.424	11	14.25	1.213
12	6.077	-0.487	12	14.26	1.215
13	5.480	-0.611	13	14.18	1.198
14	5.461	-0.615	14	14.23	1.210

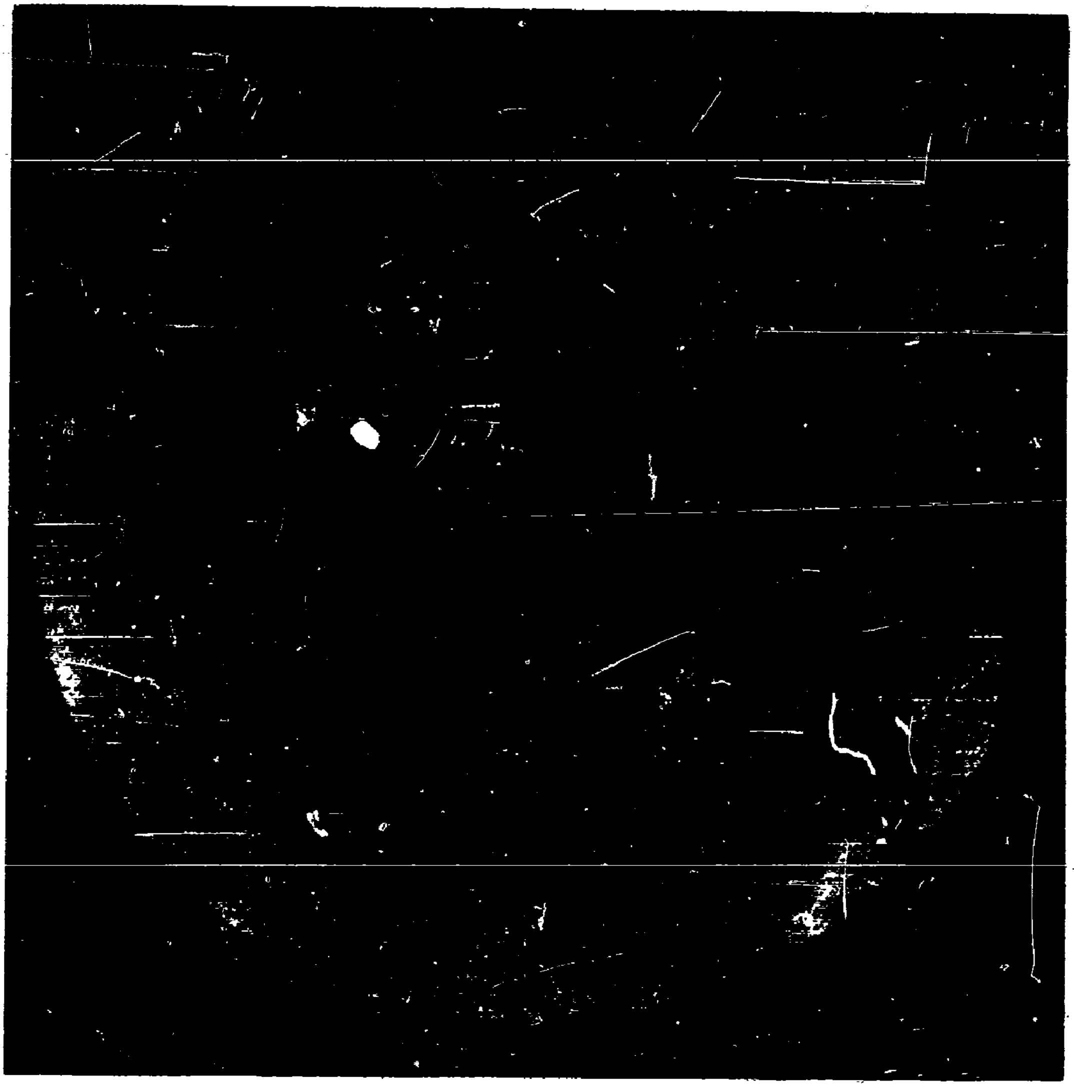

WADC TN 59-32

FIG. 19. Shadowgraph Picture of a Ribbon Parachute Model at Mach Nr. 0.946

$$C_{P_{AV}} = 1.222$$

$$\frac{P_0 - P_\infty}{q} = f(M) = 1.247$$

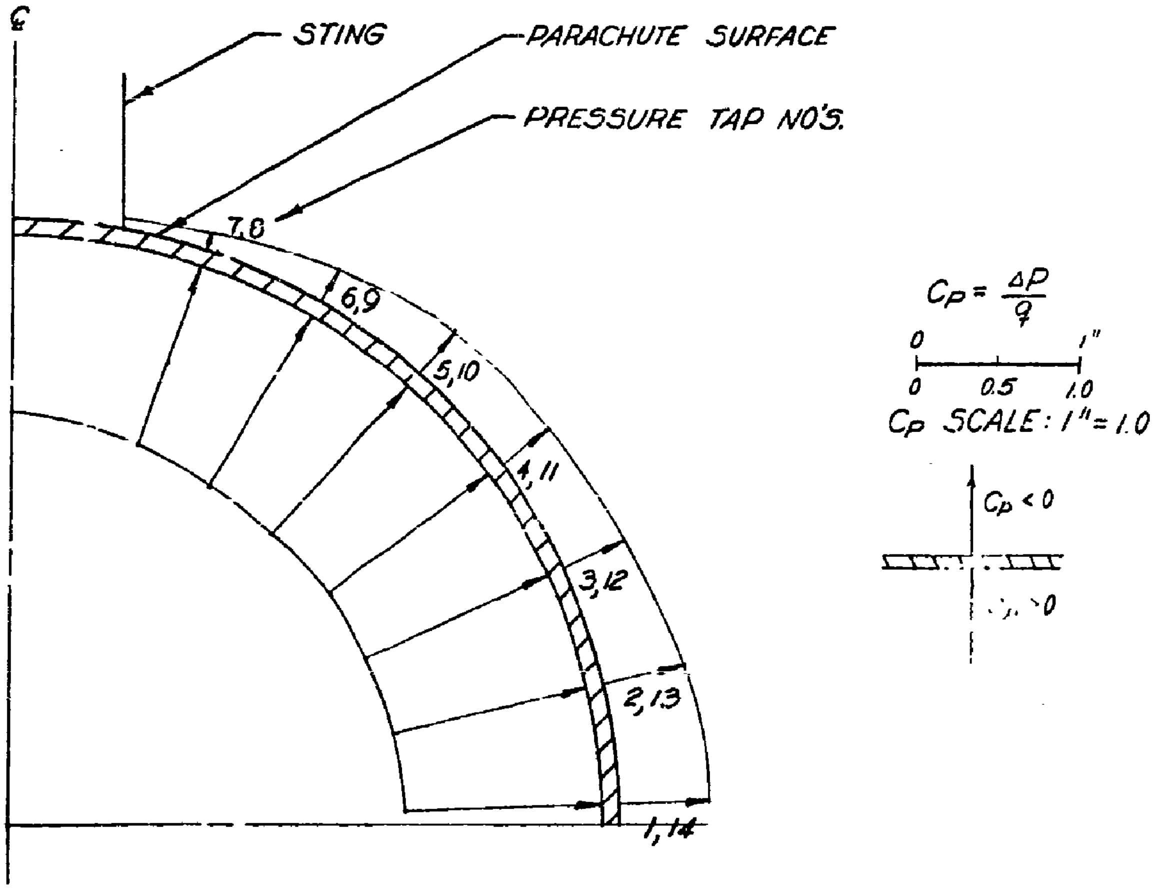

HALF MODEL OF
RIBBON PARACHUTE
SCALE : 3" = 1"

PRESSURE DISTRIBUTION ON A 2.5"
RIBBON PARACHUTE $M_\infty \simeq 0.95$

TABLE NO. 4

RIBBON TYPE PARACHUTE PRESSURE DISTRIBUTION

$M_{\infty_{AV}}$ = 0.95

EXTERNAL PRESSURE TEST M_∞ = 0.951 P_∞ = 7.995 psia, t = 72.9° F P_0 = 14.309 psia, Re = 9.28×10^5			INTERNAL PRESSURE TEST M_∞ = 0.956 P_∞ = 7.951 psia, t = 71° F P_0 = 14.312 psia, Re = 9.32×10^5		
TAP NO.	P_L (psia)	C_p	TAP NO.	P_L (psia)	C_p (+)
1	5.250	-0.542	1	14.24	1.237
2	5.343	-0.524	2	14.17	1.222
3	5.778	-0.438	3	14.22	1.233
4	6.214	-0.352	4	14.26	1.239
5	6.268	-0.341	5	14.23	1.234
6	6.845	-0.227	6	14.22	1.232
7	7.472	-0.103	7	13.93	1.174
8	7.491	-0.100	8	13.89	1.167
9	6.733	-0.249	9	14.13	1.214
10	7.726	-0.053	10	14.26	1.249
11	6.297	-0.335	11	14.24	1.237
12	5.969	-0.400	12	14.25	1.238
13	5.392	-0.514	13	14.18	1.223
14	5.382	-0.516	14	14.23	1.235

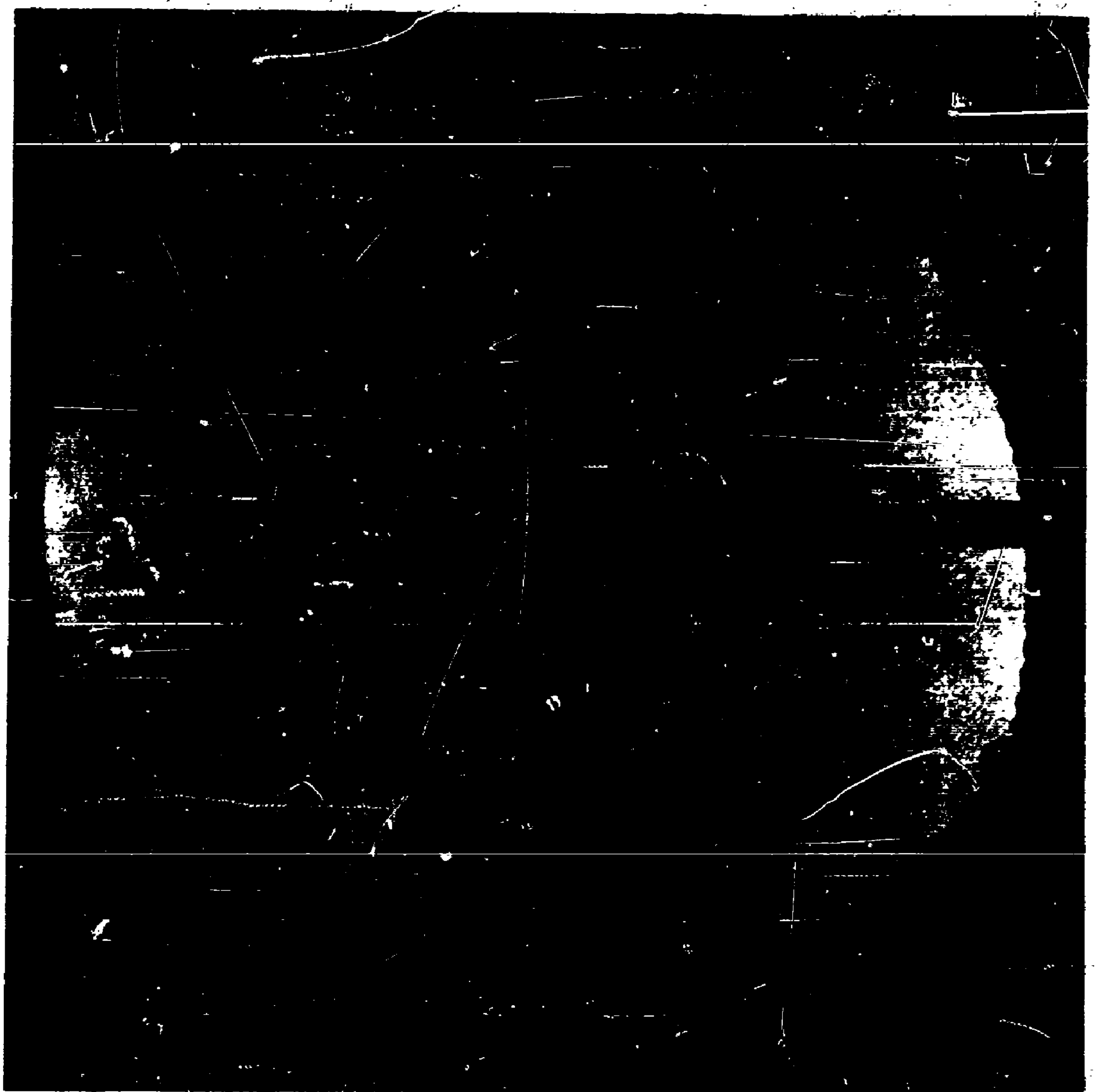

FIG. 21. Shadowgraph Picture of a Ribbon Parachute Model at Mach Nr. 1.002

$$C_{P_{AV}} = 1.259$$

$$\frac{P_0 - P_\infty}{q} = f(M) = 1.276$$

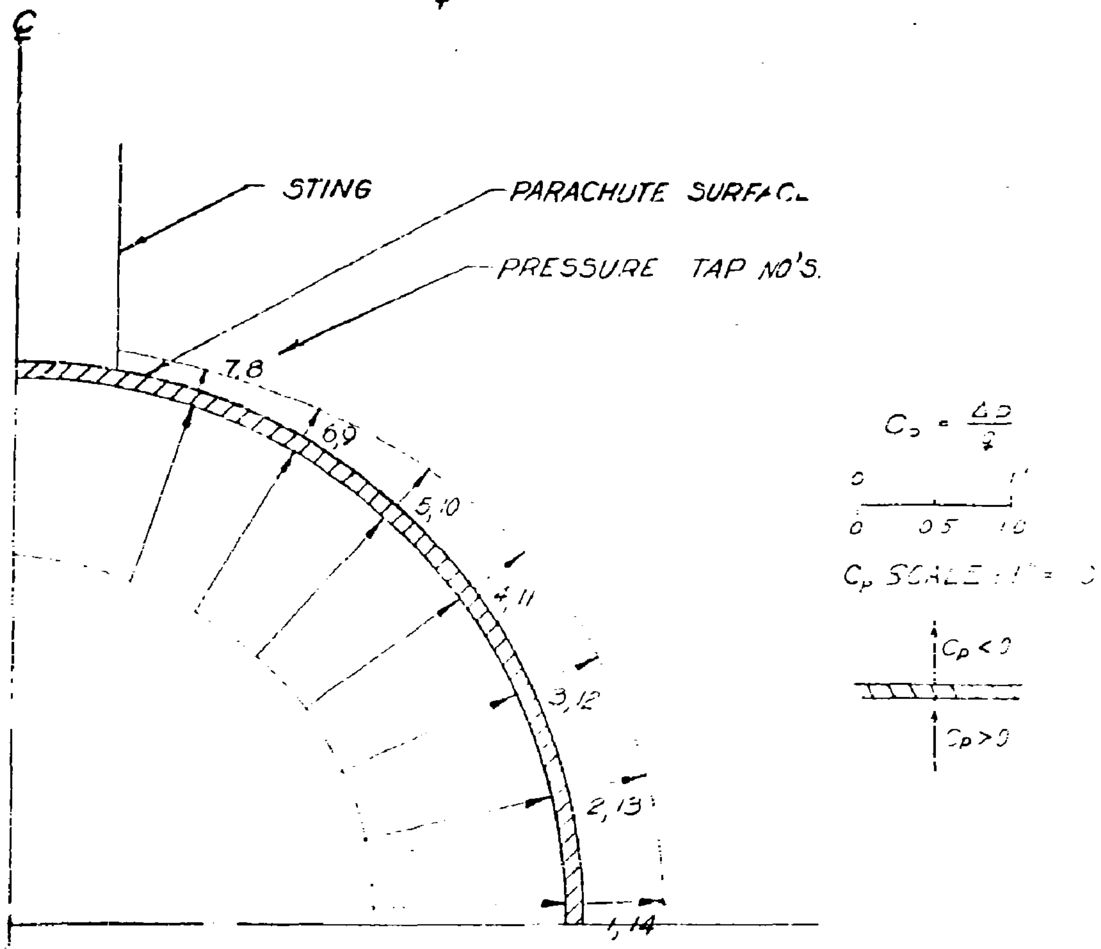

HALF MODEL OF
RIBBON PARACHUTE
SCALE : 3" = 1"

PRESSURE DISTRIBUTION ON A 2.5" RIBBON PARACHUTE $M_\infty \simeq 1.00$

FIG. 22

TABLE NO. 5

RIBBON TYPE PARACHUTE PRESSURE DISTRIBUTION

$M_{avg} = 1.00$

EXTERNAL PRESSURE TEST $M_\infty = 0.998$; $P_\infty = 7.574$ psia, $t = 72.9$ F; $P_0 = 14.309$ psia, $Re = 844 \times 10^5$			INTERNAL PRESSURE TEST $M_\infty = 1.014$; $P_\infty = 7.437$ psia, $t = 71°$ F; $P_0 = 14.312$ psia, $Re = 846 \times 10^5$		
TAP NO.	P_L (psia)	C_p	TAP NO.	P_L (psia)	$C_p(+)$
1	4.722	-0.540	1	14.25	1.273
2	4.668	-0.550	2	14.17	1.258
3	5.084	-0.472	3	14.22	1.268
4	5.475	-0.398	4	14.26	1.[illegible]74
5	5.950	-0.308	5	14.23	1.270
6	6.478	-0.208	6	14.22	1.267
7	6.904	-0.127	7	13.92	1.210
8	6.909	-0.126	8	13.89	1.205
9	6.336	-0.234	9	14.14	1.251
10	7.061	-0.097	10	14.27	1.276
11	5.622	-0.370	11	14.25	1.273
12	5.255	-0.439	12	14.26	1.274
13	4.790	-0.527	13	14.18	1.259
14	4.908	-0.505	14	14.24	1.271

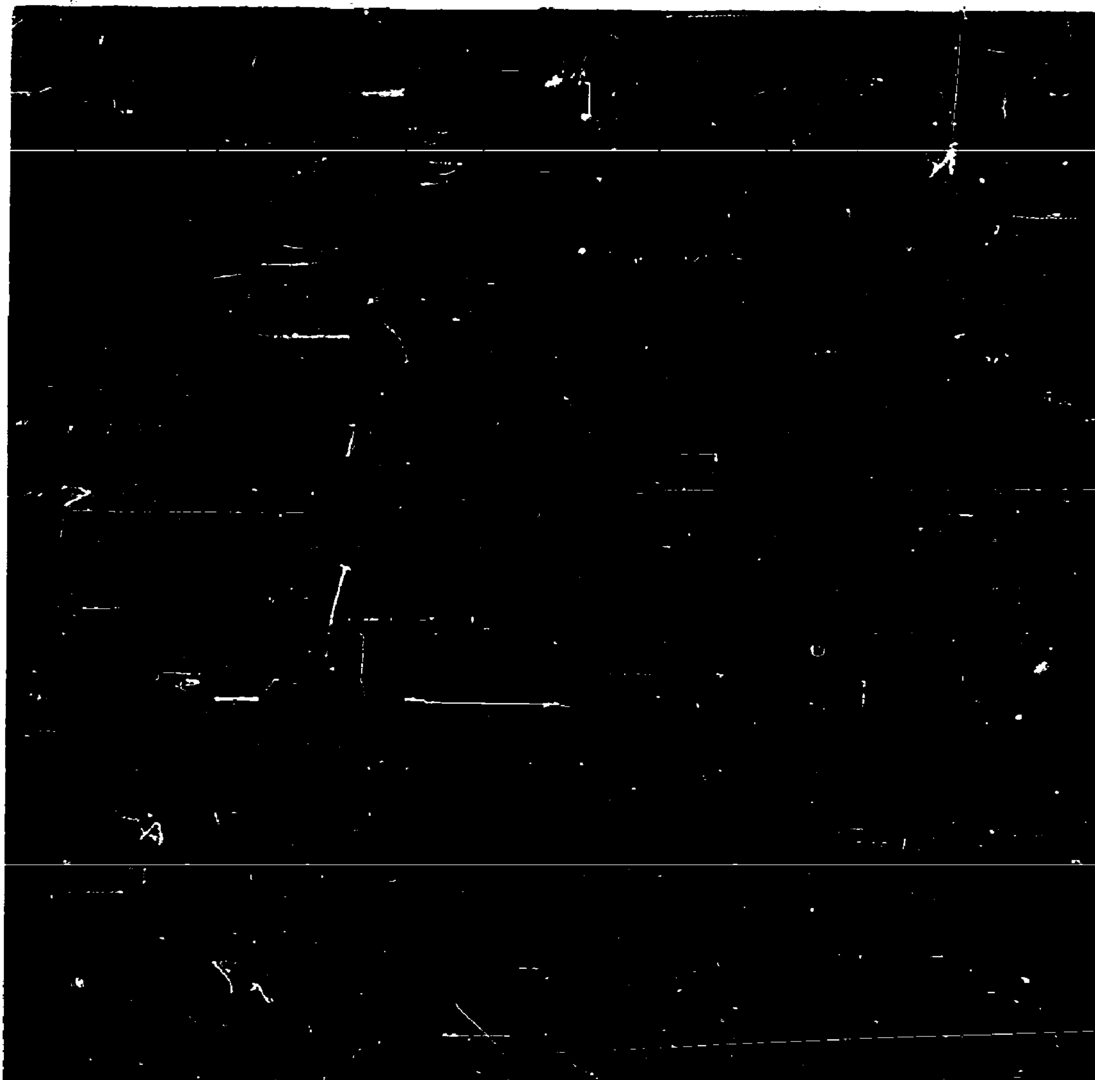

FIG. 23. Shadowgraph Picture of a Ribbon Parachute Model at Mach Nr. 1.063

$$C_{P_{AV}} = 1.288$$

$$\frac{P_0 - P_\infty}{q} = f(M) = 1.313$$

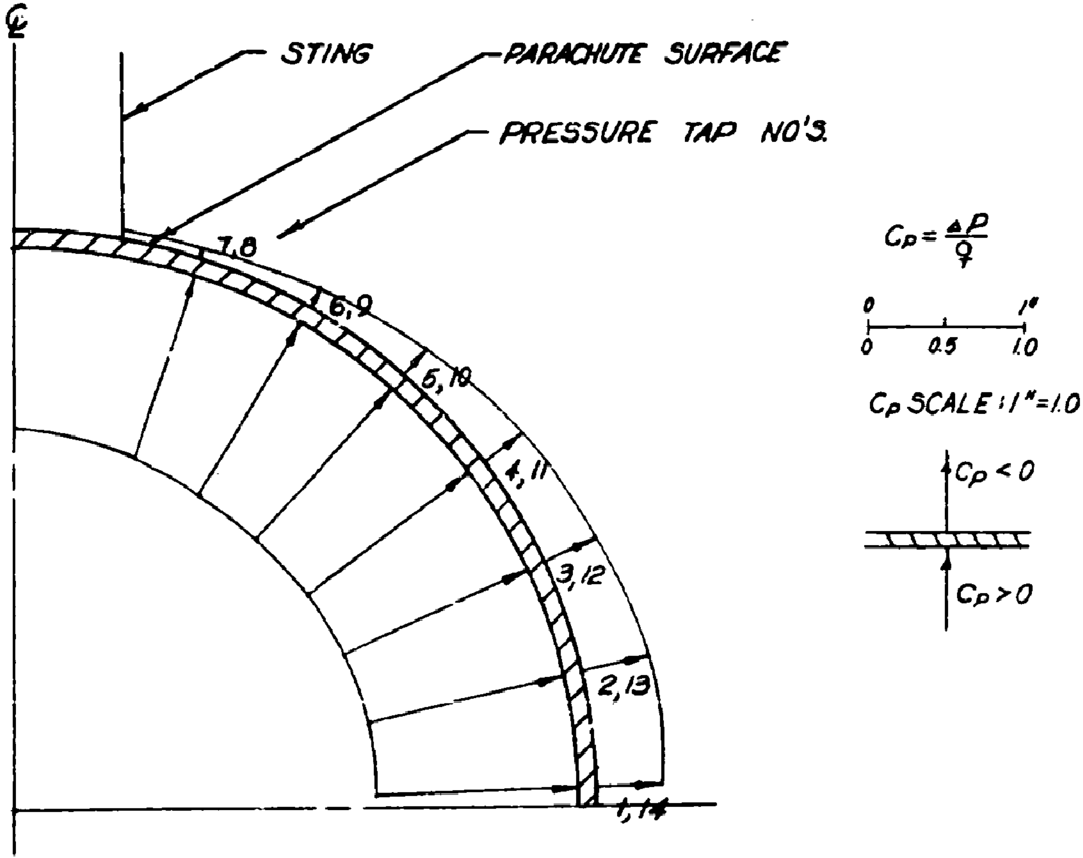

HALF MODEL OF
RIBBON PARACHUTE
SCALE : 3" = 1"

PRESSURE DISTRIBUTION ON A 2.5"
RIBBON PARACHUTE $M_\infty \simeq 1.06$

FIG. 24

TABLE NO. 6

RIBBON TYPE PARACHUTE PRESSURE DISTRIBUTION

$M_{\infty_{AV}} = 1.06$

EXTERNAL PRESSURE TEST			INTERNAL PRESSURE TEST		
$M_{\infty} = 1.061$			$M_{\infty} = 1.063$		
$P_{\infty} = 7.031$ psia		$t = 72.9°F$	$P_{\infty} = 7.017$ psia		$t = 71°F$
$P_0 = 14.309$ psia		$Re = 9.46 \times 10^5$	$P_0 = 14.312$ psia		$Re = 9.53 \times 10^5$
TAP NO.	P_L (psia)	C_p	TAP NO.	P_L (psia)	C_p (+)
1	4.619	-0.435	1	14.24	1.302
2	4.472	-0.462	2	14.16	1.287
3	4.873	-0.390	3	14.21	1.296
4	5.294	-0.314	4	14.24	1.302
5	5.754	-0.231	5	14.21	1.297
6	6.341	-0.125	6	14.21	1.296
7	6.752	-0.050	7	13.90	1.240
8	6.762	-0.049	8	13.87	1.235
9	6.175	-0.155	9	14.12	1.280
10	6.924	-0.019	10	14.25	1.303
11	5.451	-0.285	11	14.23	1.301
12	5.108	-0.347	12	14.24	1.302
13	4.624	-0.435	13	14.16	1.287
14	4.780	-0.406	14	14.23	1.300

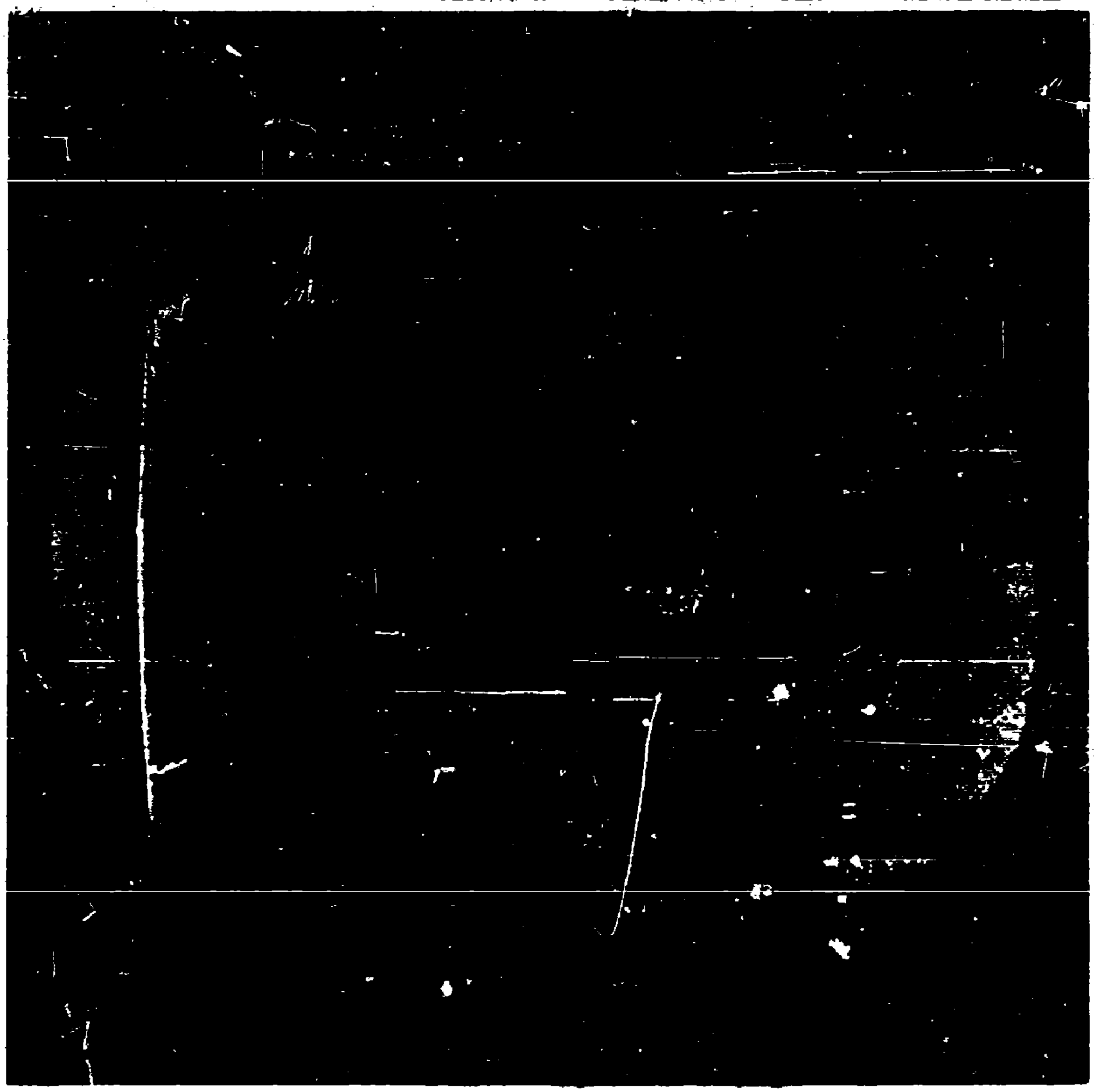

WADC TN 59-32 FIG. 25. Shadowgraph Picture of a Ribbon Parachute Model at Mach Nr. 1.131

$C_{P_{AV}} = 1.319$

$\frac{P_0 - P_\infty}{q} = f(M) = 1.354$

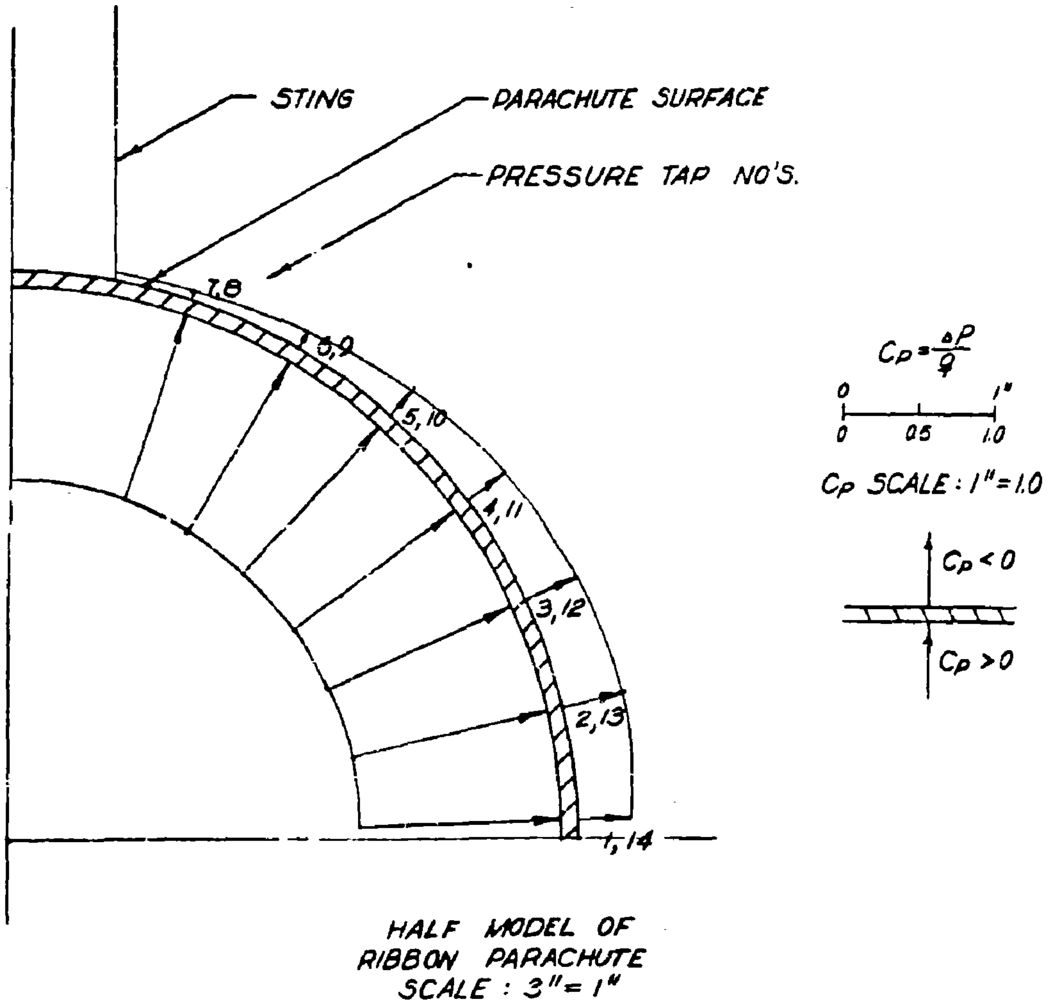

PRESSURE DISTRIBUTION ON A 2.5"
RIBBON PARACHUTE $M_\infty \simeq 1.12$

TABLE NO. 7

RIBBON TYPE PARACHUTE PRESSURE DISTRIBUTION

$M_{\infty_N} = 1.12$

EXTERNAL PRESSURE TEST $M_\infty = 1.128$ $P_\infty = 6.469$ psia $t = 72.9°F$ $P_0 = 14.309$ psia $Re = 9.53 \times 10^5$			INTERNAL PRESSURE TEST $M_\infty = 1.115$ $P_\infty = 6.581$ psia $t = 71°F$ $P_0 = 14.312$ psia $Re = 9.65 \times 10^5$		
TAP NO.	P_L (psia)	C_p	TAP NO.	P_L (psia)	C_p (+)
1	4.472	-0.347	1	14.20	1.331
2	3.993	-0.430	2	14.13	1.318
3	4.325	-0.372	3	14.17	1.326
4	4.541	-0.335	4	14.21	1.332
5	4.991	-0.257	5	14.18	1.328
6	5.779	-0.120	6	14.19	1.329
7	6.214	-0.044	7	13.85	1.270
8	6.219	-0.043	8	13.82	1.265
9	5.823	-0.112	9	14.09	1.311
10	6.195	-0.048	10	14.21	1.333
11	4.834	-0.284	11	14.20	1.331
12	4.521	-0.338	12	14.21	1.332
13	4.130	-0.406	13	14.13	1.318
14	4.536	-0.336	14	14.18	1.328

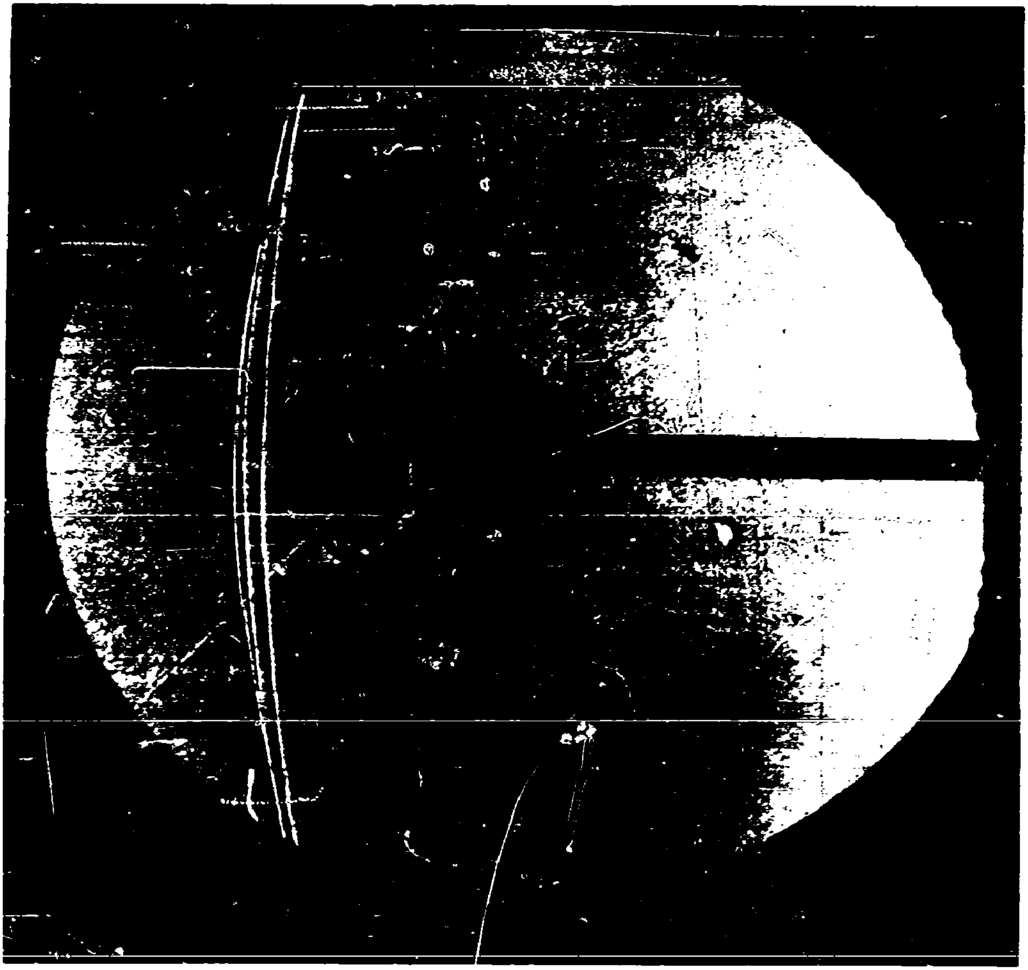

FIG. 27. Shadowgraph Picture of a Ribbon Parachute Model at Mach Nr. 1.194

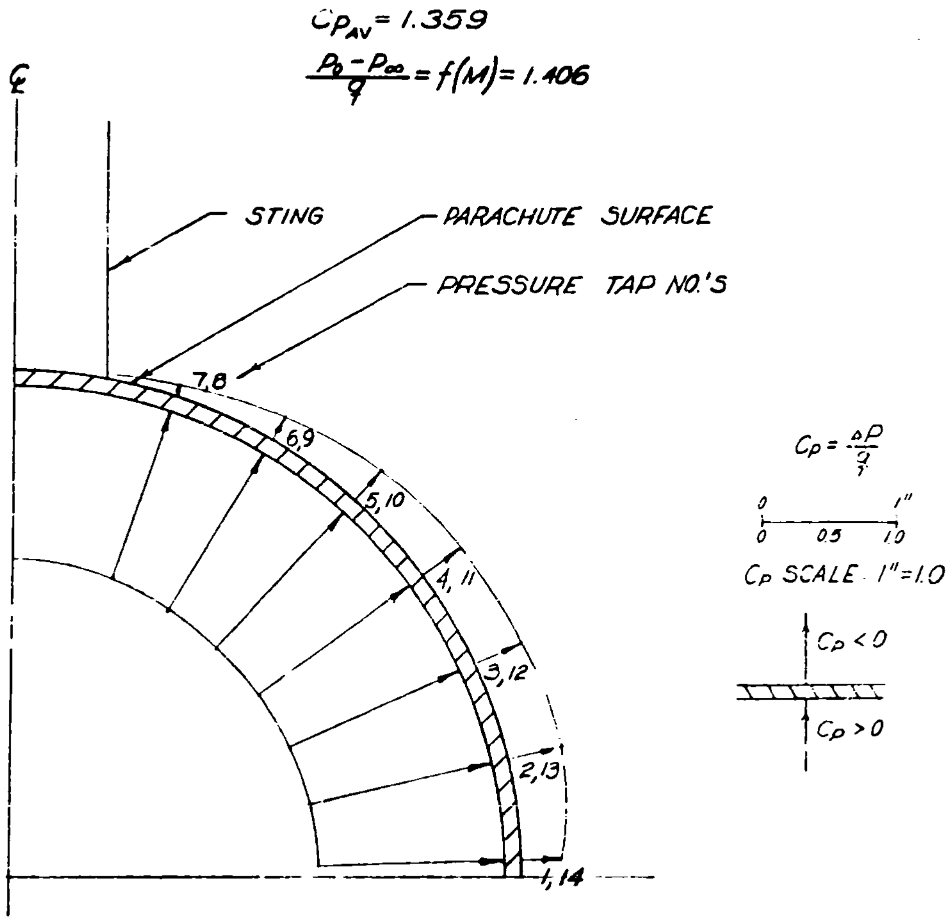

HALF MODEL OF
RIBBON PARACHUTE
SCALE : 3" = 1"

PRESSURE DISTRIBUTION ON A 2.5" RIBBON PARACHUTE $M_\infty \simeq 1.19$

TABLE NO. 8

RIBBON TYPE PARACHUTE PRESSURE DISTRIBUTION

$M_{\infty_{AV}} = 1.19$

EXTERNAL PRESSURE TEST $M_\infty = 1.191$ $P_\infty = 5.969$ psia $t = 72.9°F$ $P_0 = 14.309$ psia $Re = 9.59 \times 10^5$			INTERNAL PRESSURE TEST $M_\infty = 1.192$ $P_\infty = 5.965$ psia $t = 71°F$ $P_0 = 14.312$ psia $Re = 9.69 \times 10^5$		
TAP NO.	P_L (psia)	C_p	TAP NO.	P_L (psia)	C_p (+)
1	4.242	-0.291	1	14.11	1.373
2	3.454	-0.424	2	14.02	1.357
3	3.640	-0.394	3	14.08	1.367
4	3.699	-0.383	4	14.11	1.373
5	4.188	-0.301	5	14.09	1.368
6	4.619	-0.228	6	14.08	1.368
7	5.534	-0.074	7	13.74	1.311
8	5.578	-0.066	8	13.72	1.307
9	4.864	-0.187	9	13.99	1.352
10	5.333	-0.107	10	14.12	1.374
11	4.051	-0.324	11	14.10	1.371
12	3.797	-0.367	12	14.11	1.373
13	3.577	-0.404	13	14.02	1.358
14	4.247	-0.291	14	14.09	1.369

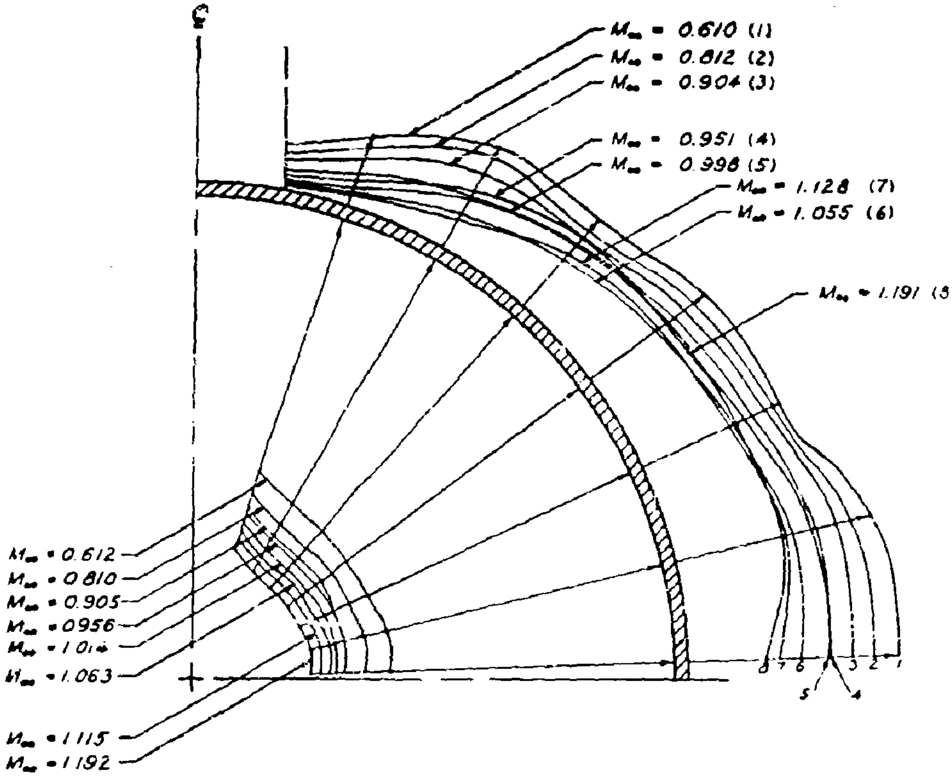

MODEL SCALE : 3" = 1"

C_p SCALE : 1" = 0.50

SUMMARY OF C_p DISTRIBUTION FOR A $2\frac{1}{2}$ IN. DIAMETER RIBBON PARACHUTE MODEL
AVERAGED VALUES OF C_p PLOTTED ON HALF MODEL

FIG. 29

FIGURE 39. SHADOWGRAPH PICTURE OF A GUIDE SURFACE PARACHUTE MODEL AT MACH NUMBER 0.615.

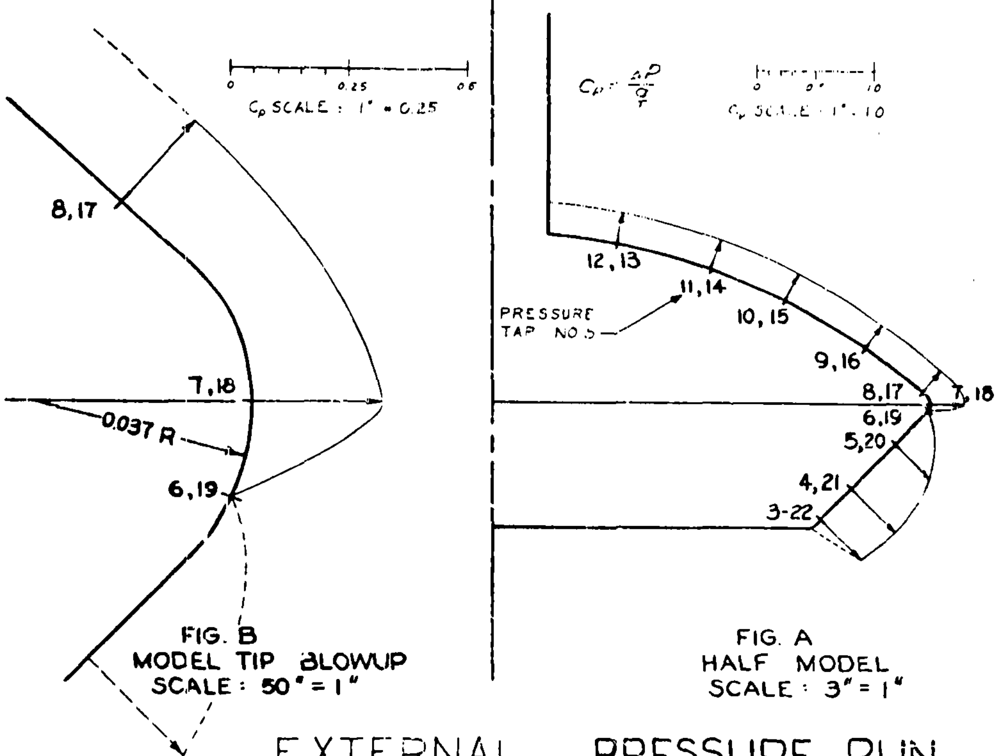

FIG. B
MODEL TIP BLOWUP
SCALE : 50" = 1"

FIG. A
HALF MODEL
SCALE : 3" = 1"

EXTERNAL PRESSURE RUN
RUN NO. 1 C_p DISTRIBUTION ON
$2\frac{1}{2}$" GUIDE SURFACE PARACHUTE $M_\infty = 0.615$

FIG. 31

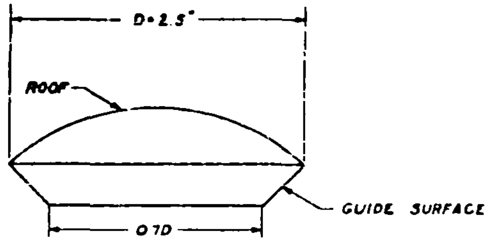

FIG. A
FULL SCALE MODEL OF
GUIDE SURFACE PARACHUTE

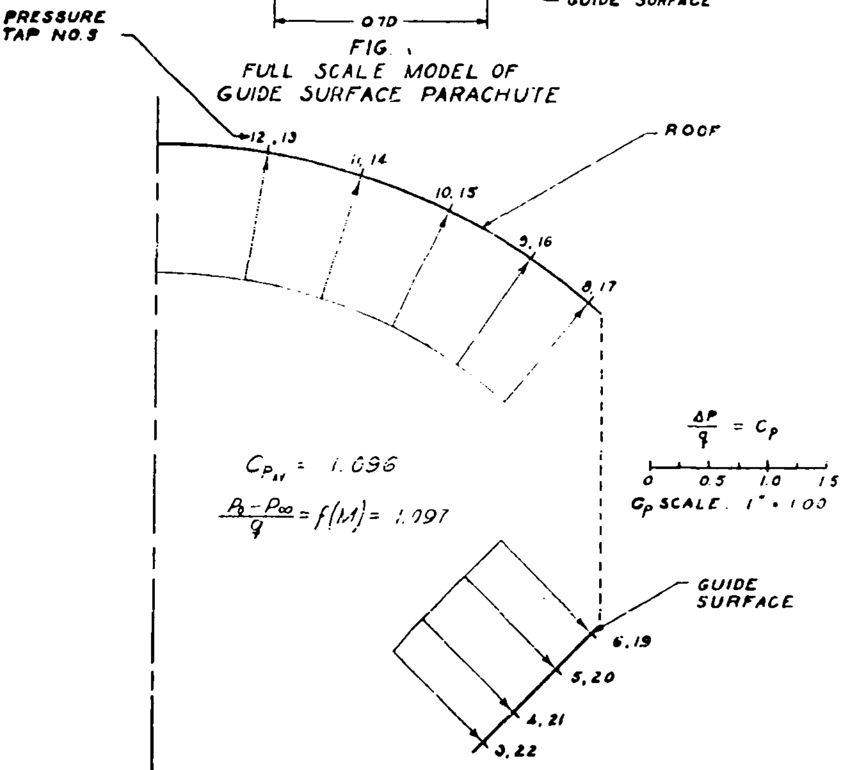

FIG. B
HALF MODEL : SURFACES DETACHED
SCALE : 3" = 1"

INTERNAL PRESSURE TEST
RUN NO. 9 C_p DISTRIBUTION ON
$2\frac{1}{2}$" GUIDE SURFACE PARACHUTE
$M_\infty = 0.612$
FIG. 32

TABLE NO. 9.

GUIDE SURFACE PARACHUTE PRESSURE DISTRIBUTION

M_{∞_M} = 0.61

EXTERNAL PRESSURE TEST M_{∞} = 0.615 P_{∞} = 11.032 psia, t = 72° F P_0 = 14.241 psia, R_e = 7.26 × 10^5			INTERNAL PRESSURE TEST M_{∞} = 0.612 P_{∞} = 11.125 psia, t = 94° F P_0 = 14.325 psia, R_e = 6.99 × 10^5		
TAP NO.	P_L (psia)	C_p	TAP NO.	P_L (psia)	C_p (+)
3	9.599	-0.491	3	14.187	1.050
4	9.531	-0.514	4	14.319	1.095
5	9.819	-0.415	5	14.329	1.099
6	11.018	-0.005	6	14.329	1.099
7	10.167	-0.297	7	14.334	1.100
8	10.367	-0.228	8	14.329	1.099
9	10.338	-0.238	9	14.324	1.097
10	10.318	-0.244	10	14.324	1.097
11	10.313	-0.246	11	14.334	1.100
12	10.294	-0.253	12	14.334	1.100
13	10.304	-0.249	13	14.329	1.099
14	10.309	-0.248	14	14.334	1.100
15	10.323	-0.243	15	14.319	1.095
16	10.348	-0.234	16	14.329	1.099
17	10.377	-0.224	17	14.329	1.099
18	10.299	-0.251	18	14.338	1.102
19	11.052	+0.007	19	14.334	1.100
20	9.937	-0.375	20	14.324	1.097
21	9.565	-0.502	21	14.329	1.099
22	9.658	-0.471	22	14.324	1.097

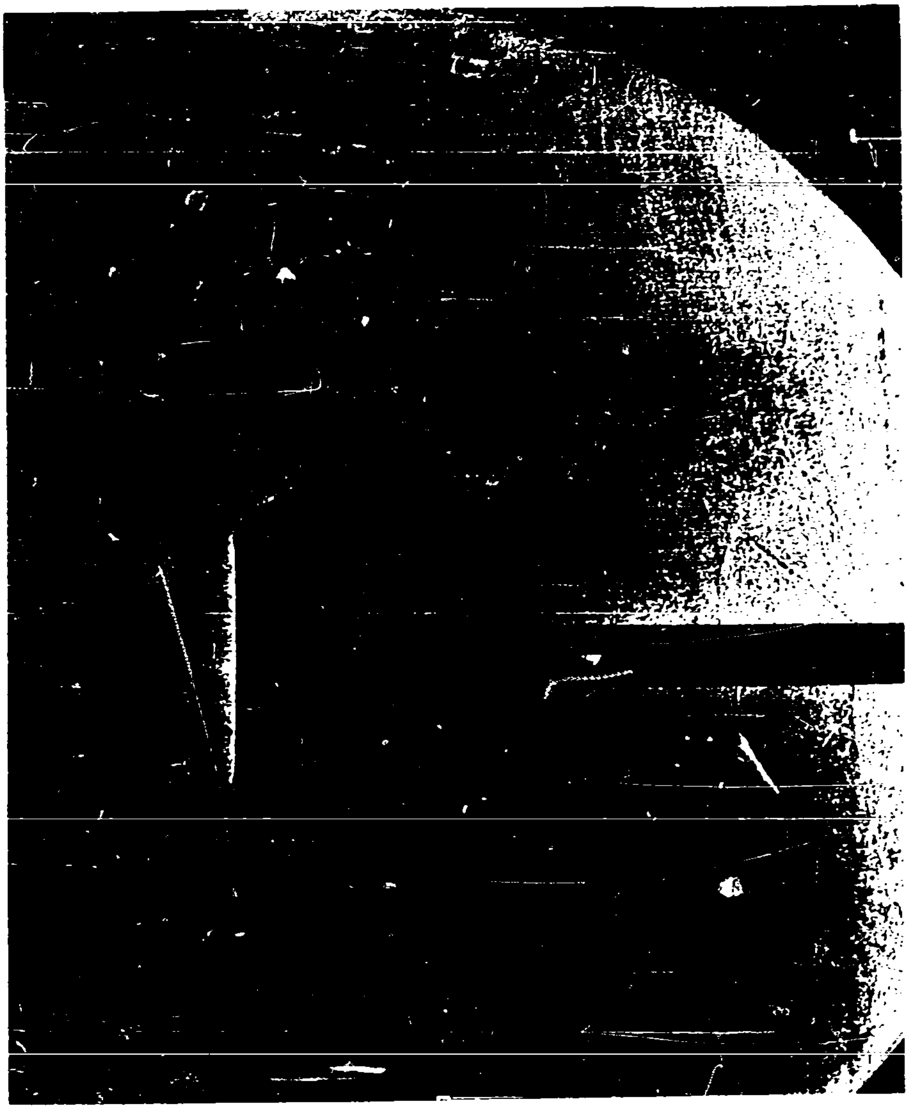

FIGURE 3-. SHADOWGRAPH PICTURE OF A GUIDE SURFACE PARACHUTE MODEL AT MACH NUMBER 0.805.

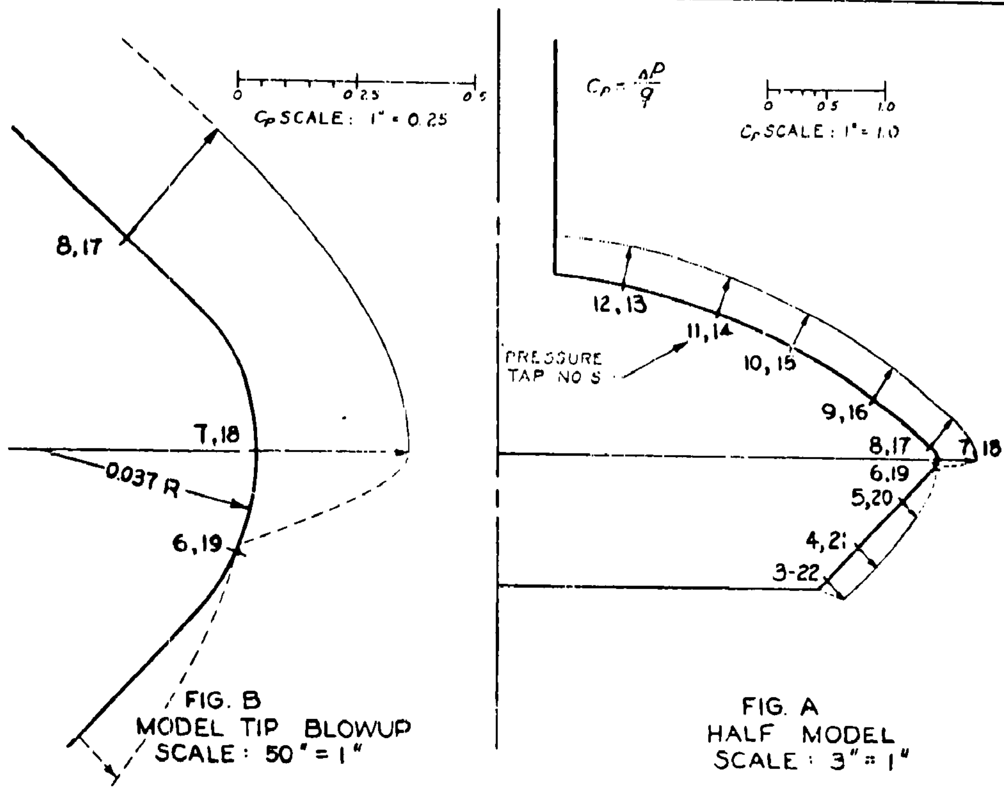

EXTERNAL PRESSURE RUN
RUN NO. 2 C_P DISTRIBUTION ON
$2\frac{1}{2}$" GUIDE SURFACE PARACHUTE $M_\infty = 0.805$

FIG. 34

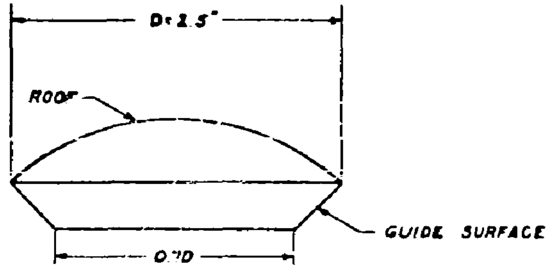

FIG. A
FULL SCALE MODEL OF
GUIDE SURFACE PARACHUTE

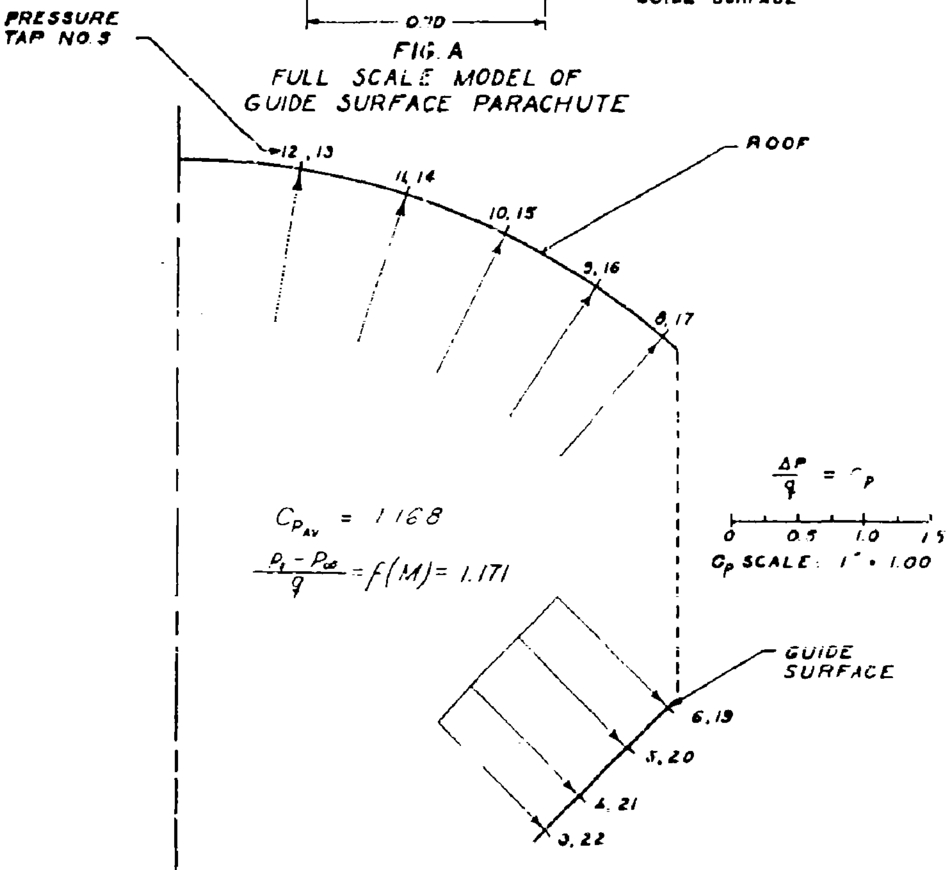

FIG. B
HALF MODEL: SURFACES DETACHED
SCALE: 3" = 1"

INTERNAL PRESSURE TEST
RUN NO. 10 C_p DISTRIBUTION ON
$2\frac{1}{2}$" GUIDE SURFACE PARACHUTE
$M_\infty = 0.801$
FIG. 35

TABLE NO. 10

GUIDE SURFACE PARACHUTE PRESSURE DISTRIBUTION

$M_{\infty} = 0.80$

EXTERNAL PRESSURE TEST			INTERNAL PRESSURE TEST		
$M_{\infty} = 0.805$			$M_{\infty} = 0.801$		
$P_{\infty} = 9.294$ psia	$t = 72°$ F		$P_{\infty} = 9.365$ psia	$t = 94°$ F	
$P_0 = 14.237$ psia	$R_e = 8.63 \times 10^5$		$P_0 = 14.321$ psia	$R_e = 8.20 \times 10^5$	
TAP NO.	P_i (psia)	C_p	TAP NO.	P_i (psia)	C_p (+)
3	7.437	-0.441	3	14.120	1.124
4	7.368	-0.457	4	14.301	1.167
5	7.716	-0.374	5	14.316	1.171
6	9.272	-0.005	6	14.316	1.171
7	7.892	-0.333	7	14.321	1.172
8	8.127	-0.277	8	14.316	1.171
9	8.102	-0.283	9	14.311	1.169
10	8.073	-0.290	10	14.311	1.169
11	8.063	-0.292	11	14.321	1.172
12	8.039	-0.298	12	14.321	1.178
13	8.044	-0.297	13	14.316	1.171
14	8.063	-0.292	14	14.321	1.172
15	8.068	-0.291	15	14.311	1.169
16	8.093	-0.285	16	14.316	1.171
17	8.097	-0.284	17	14.321	1.172
18	8.044	-0.297	18	14.326	1.173
19	9.360	+0.016	19	14.321	1.172
20	7.897	-0.332	20	14.311	1.169
21	7.398	-0.450	21	14.316	1.171
22	7.500	-0.426	22	14.306	1.168

FIGURE 36. SHADOWGRAPH PICTURE OF A GUIDE SURFACE PARACHUTE MODEL AT MACH NUMBER 0.890.

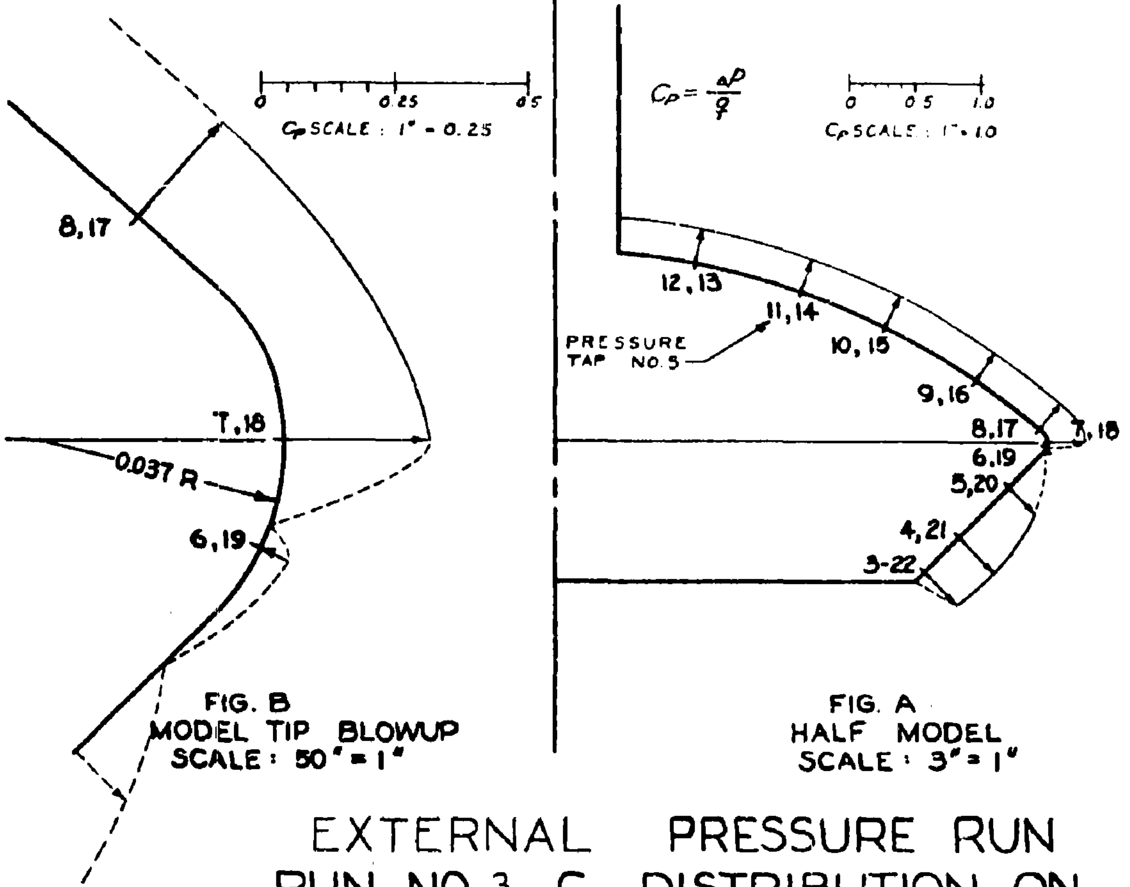

FIG. B
MODEL TIP BLOWUP
SCALE: 50" = 1"

FIG. A
HALF MODEL
SCALE: 3" = 1"

EXTERNAL PRESSURE RUN
RUN NO. 3 C_p DISTRIBUTION ON
$2\frac{1}{2}$" GUIDE SURFACE PARACHUTE $M_\infty = 0.890$

X FIG. 37

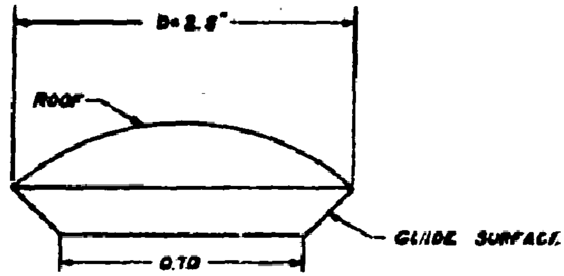

FIG. A
FULL SCALE MODEL OF
GUIDE SURFACE PARACHUTE

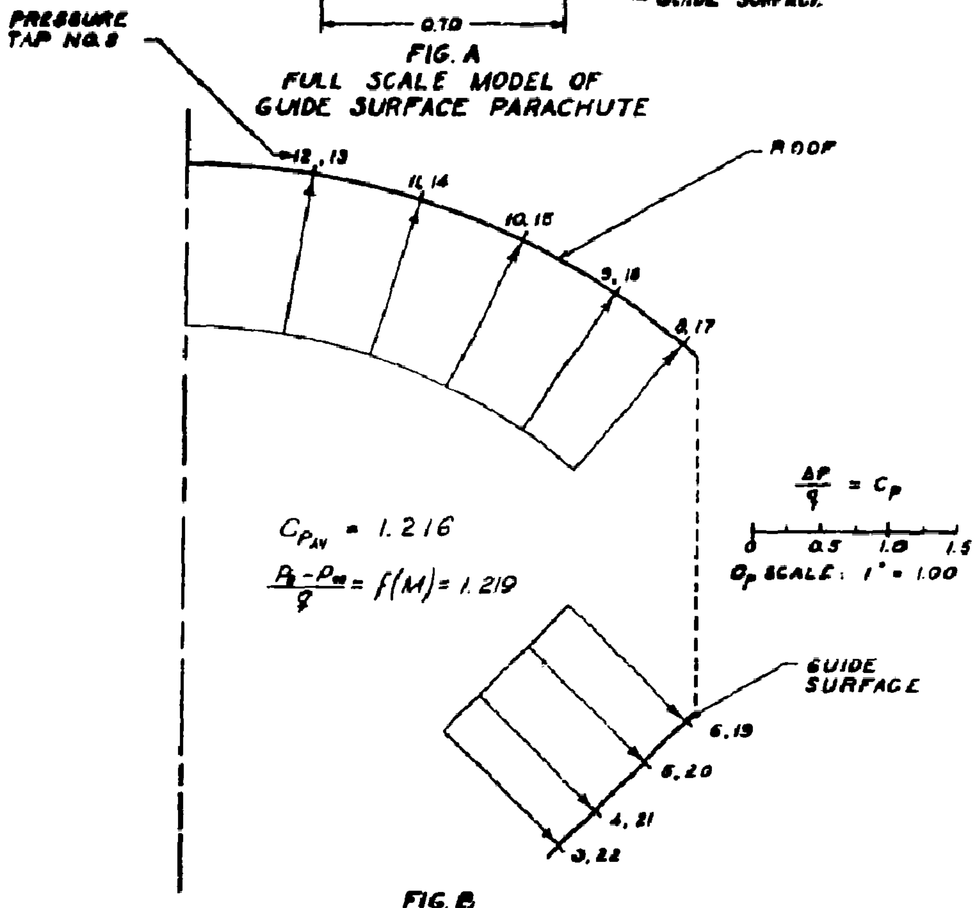

FIG. B
HALF MODEL: SURFACES DETACHED
SCALE: 3" = 1"

INTERNAL PRESSURE TEST
RUN NO. 11 C_p DISTRIBUTION ON
$2\frac{1}{2}$" GUIDE SURFACE PARACHUTE
$M_\infty = 0.899$
FIG. 38

TABLE NO 11

GUIDE SURFACE PARACHUTE PRESSURE DISTRIBUTION

$M_{\infty_{nom}}$ = .89

EXTERNAL PRESSURE TEST			INTERNAL PRESSURE TEST		
M_∞ = 0.890			M_∞ = 0.899		
P_∞ = 8.509 psia	t = 72° F		P_∞ = 8.477 psia	t = 114° F	
P_0 = 14.237 psia	R_e = 9.05×10^5		P_0 = 14.321 psia	R_e = 8.65×10^5	
TAP NO.	P_L (psia)	C_p	TAP NO.	P_L (psia)	C_p (+)
3	6.847	-0.352	3	14.105	1.174
4	6.673	-0.368	4	14.311	1.217
5	7.145	-0.289	5	14.320	1.219
6	8.701	+0.041	6	14.320	1.219
7	7.150	-0.288	7	14.325	1.220
8	7.395	-0.236	8	14.320	1.219
9	7.370	-0.242	9	14.311	1.217
10	7.341	-0.248	10	14.315	1.218
11	7.326	-0.251	11	14.325	1.220
12	7.317	-0.253	12	14.325	1.220
13	7.302	-0.256	13	14.320	1.219
14	7.321	-0.252	14	14.325	1.220
15	7.326	-0.251	15	14.315	1.218
16	7.361	-0.244	16	14.315	1.218
17	7.395	-0.236	17	14.320	1.219
18	7.317	-0.253	18	14.325	1.220
19	8.833	+0.069	19	14.325	1.220
20	7.365	-0.242	20	14.3[illegible]	1.217
21	6.832	-0.356	21	14.315	1.218
22	6.940	-0.333	22	14.311	1.217

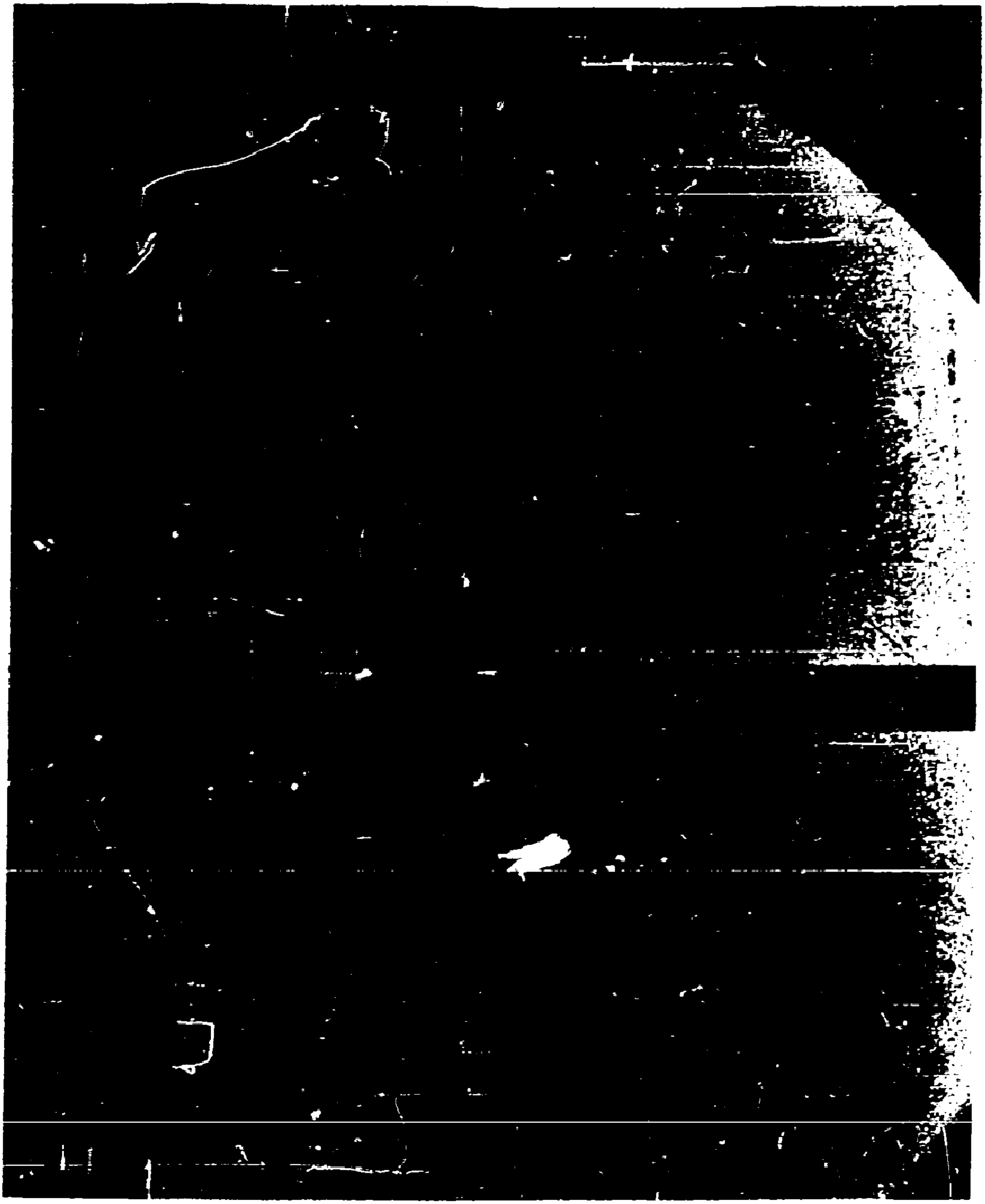

FIGURE 39. SHADOWGRAPH PICTURE OF A GUIDE SURFACE PARACHUTE MODEL AT MACH NUMBER 0.930.

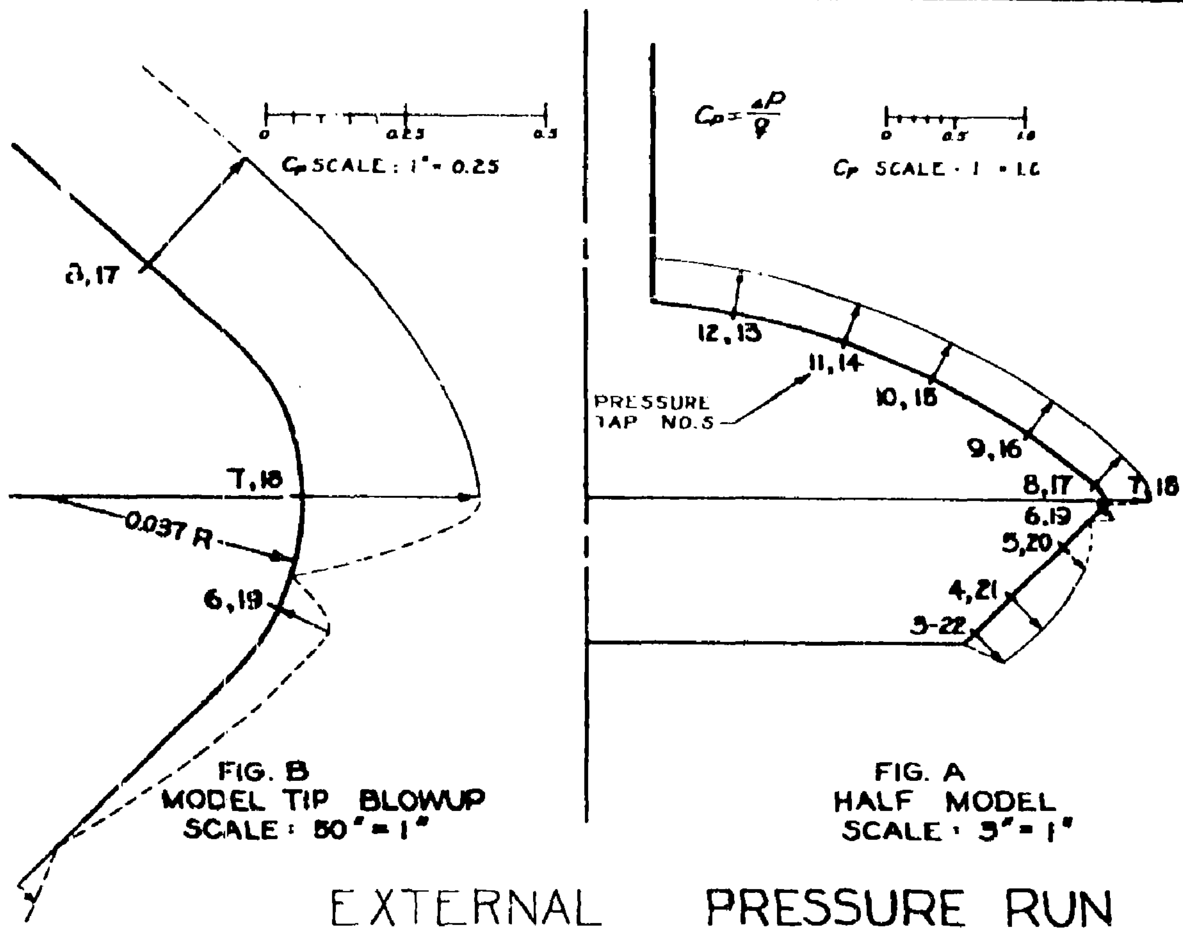

EXTERNAL PRESSURE RUN
RUN NO. 4 C_p DISTRIBUTION ON
$2\frac{1}{2}$" GUIDE SURFACE PARACHUTE $M_\infty = 0.930$

FIG. 40

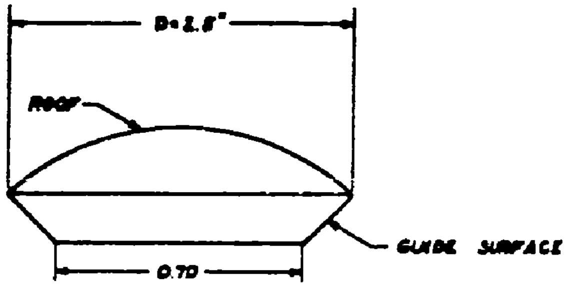

FIG. A
FULL SCALE MODEL OF
GUIDE SURFACE PARACHUTE

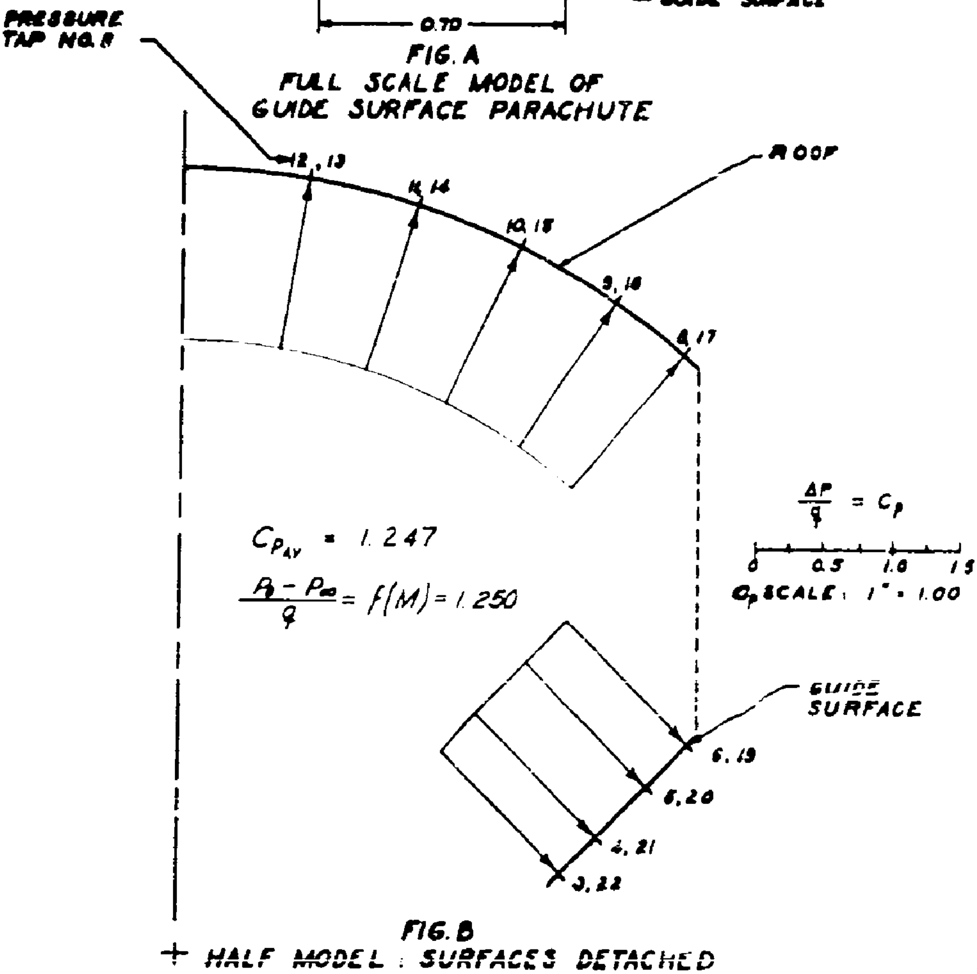

FIG. B
HALF MODEL : SURFACES DETACHED
SCALE : 3" = 1"

INTERNAL PRESSURE TEST
RUN NO. 12 C_p DISTRIBUTION ON
$2\frac{1}{2}$" GUIDE SURFACE PARACHUTE
$M_\infty = 0.956$
FIG. 41

TABLE NO. 12

GUIDE SURFACE PARACHUTE PRESSURE DISTRIBUTION

$M_{\infty_{av}} =$ 0.94

EXTERNAL PRESSURE TEST $M_\infty = 0.930$ $P_\infty = 8.145$ psia $t = 72°$ F $P_0 = 14.237$ psia $R_e = 9.17 \times 10^5$			INTERNAL PRESSURE TEST $M_\infty = 0.956$ $P_\infty = 7.958$ psia $t = 94°$ F $P_0 = 14.321$ psia $R_e = 8.78 \times 10^5$		
TAP NO.	P_L (psia)	C_p	TAP NO.	P_L (psia)	C_p (+)
3	6.689	-0.295	3	14.107	1.208
4	6.616	-0.310	4	14.307	1.247
5	7.046	-0.223	5	14.322	1.250
6	8.588	+0.090	6	14.317	1.249
7	6.498	-0.334	7	14.328	1.251
8	6.748	-0.283	8	14.322	1.250
9	6.709	-0.291	9	14.312	1.248
10	6.694	-0.294	10	14.312	1.248
11	6.689	-0.295	11	14.317	1.249
12	6.660	-0.301	12	14.322	1.250
13	6.655	-0.302	13	14.317	1.249
14	6.679	-0.297	14	14.328	1.251
15	6.679	-0.297	15	14.317	1.249
16	6.709	-0.291	16	14.317	1.249
17	6.738	-0.285	17	14.322	1.250
18	6.670	-0.299	18	14.327	1.251
19	8.666	+0.106	19	14.322	1.250
20	7.218	-0.188	20	14.312	1.248
21	6.655	-0.302	21	14.317	1.249
22	6.759	-0.281	22	14.312	1.248

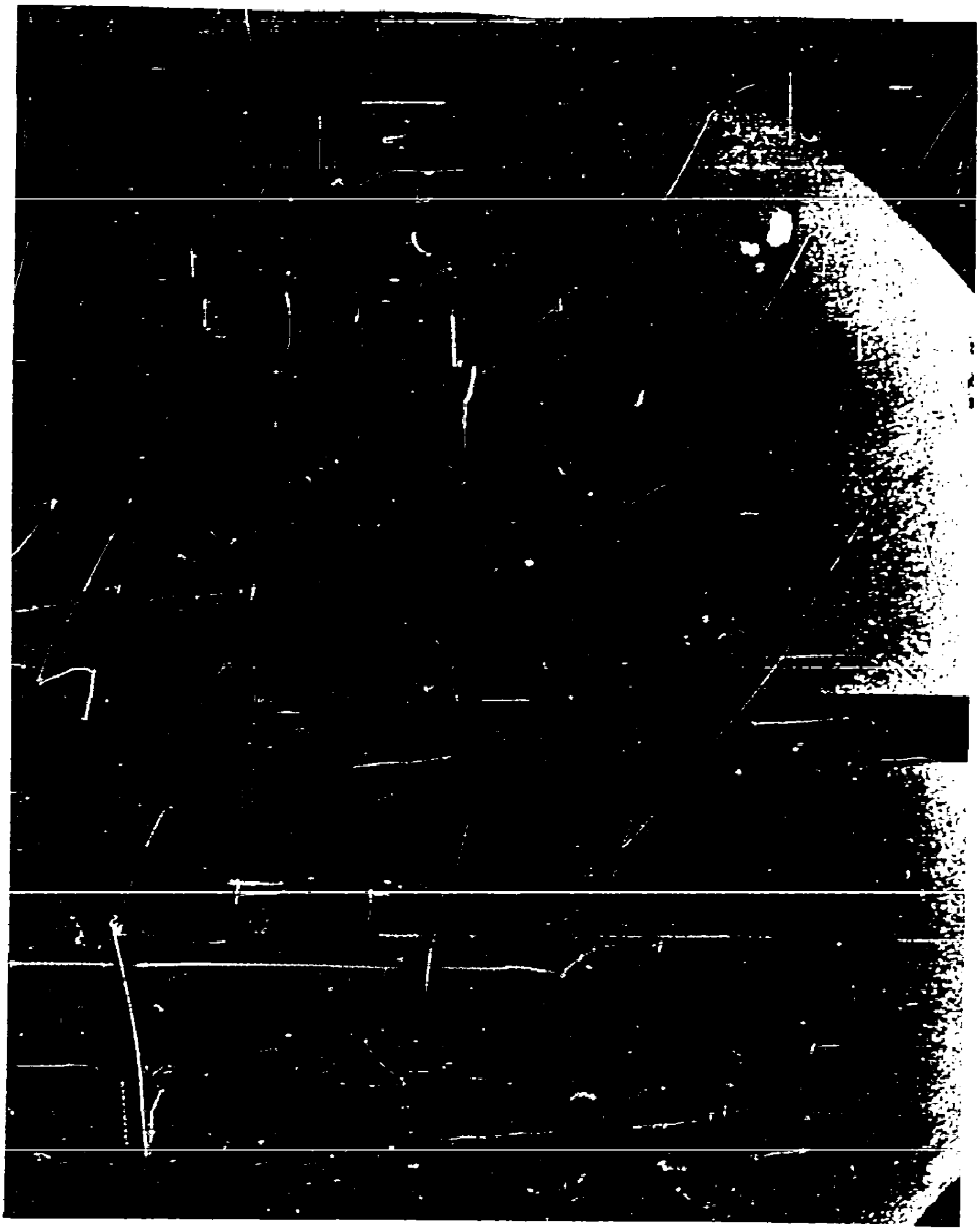

FIGURE 42. SHADOWGRAPH PICTURE OF A GUIDE SURFACE PARACHUTE MODEL AT MACH NUMBER 1.007.

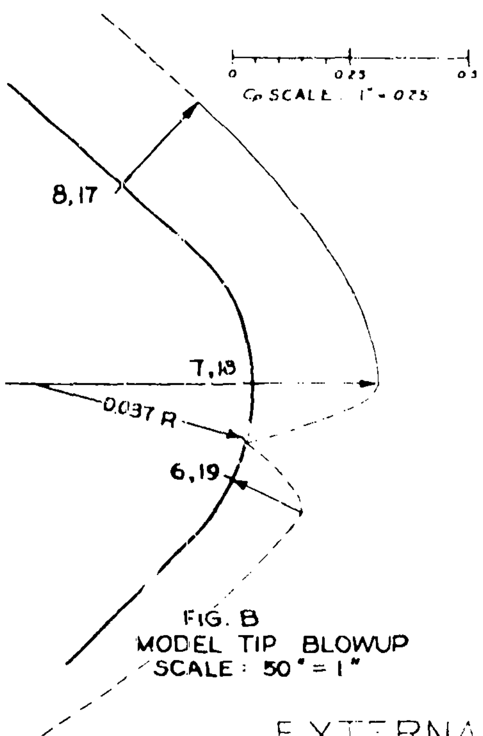

FIG. B
MODEL TIP BLOWUP
SCALE: 50" = 1"

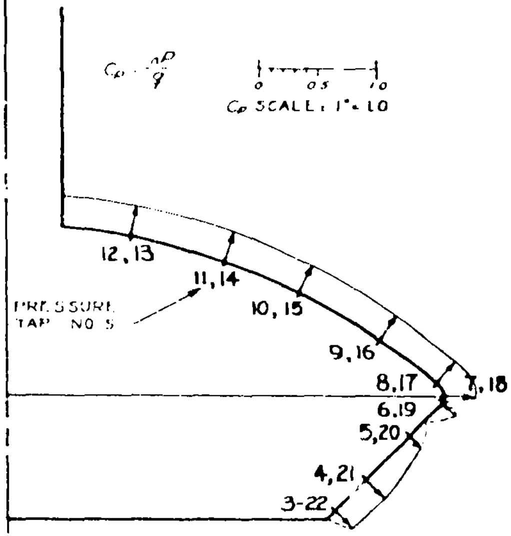

FIG. A
HALF MODEL
SCALE: 3" = 1"

EXTERNAL PRESSURE RUN
RUN NO. 5 C_p DISTRIBUTION ON
$2\frac{1}{2}$" GUIDE SURFACE PARACHUTE M_∞ = 1.007

X

FIG. 43

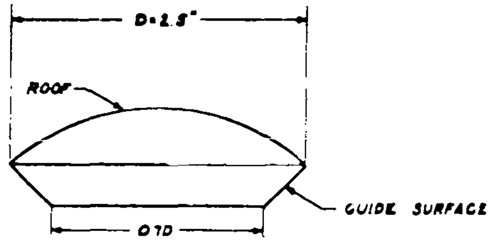

FIG. A
FULL SCALE MODEL OF
GUIDE SURFACE PARACHUTE

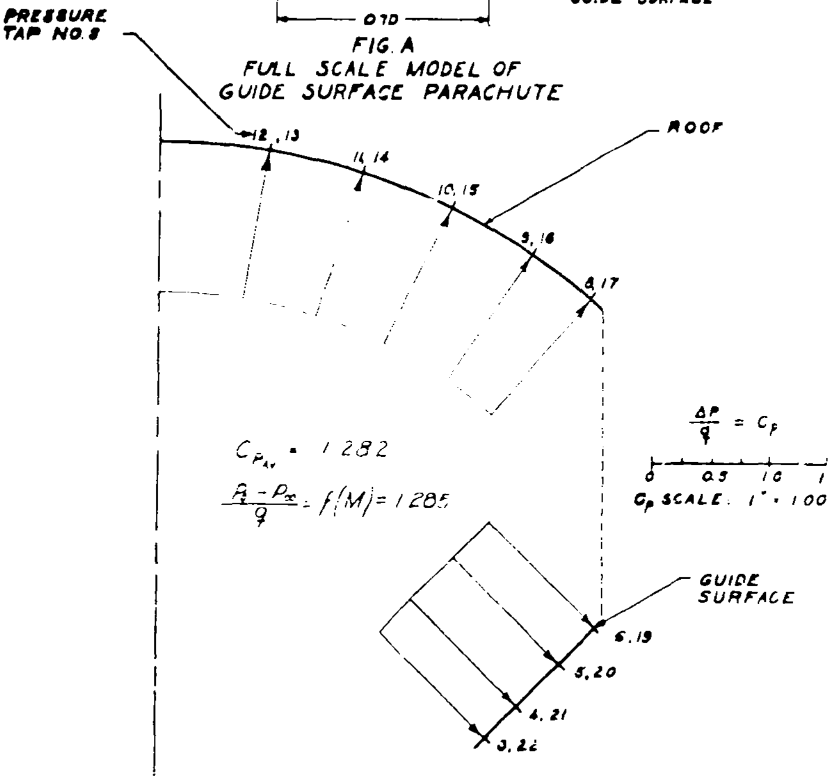

FIG. B
HALF MODEL : SURFACES DETACHED
SCALE : 3" = 1"

INTERNAL PRESSURE TEST
RUN NO. 13 C_p DISTRIBUTION ON
$2\frac{1}{2}$" GUIDE SURFACE PARACHUTE
$M_\infty = 1.015$
FIG. 44

TABLE NO. 13

GUIDE SURFACE PARACHUTE PRESSURE DISTRIBUTION

$M_{\infty_{av}}$ = 1.01

EXTERNAL PRESSURE TEST M_∞ = 1.007 P_∞ = 7.460 psia, t = 72° F P_0 = 14.237 psia, R_e = 9.44×10^5			INTERNAL PRESSURE TEST M_∞ = 1.015 P_∞ = 7.436 psia, t = 94° F P_0 = 14.327 psia, R_e = 8.99×10^5		
TAP NO.	P_L (psia)	C_P	TAP NO.	P_L (psia)	C_P (+)
3	6.363	-0.206	3	14.097	1.242
4	6.286	-0.222	4	14.308	1.281
5	6.726	-0.139	5	14.322	1.284
6	8.267	+0.152	6	14.317	1.283
7	5.968	-0.282	7	14.332	1.286
8	6.227	-0.233	8	14.322	1.284
9	6.193	-0.239	9	14.317	1.283
10	6.168	-0.244	10	14.322	1.284
11	6.173	-0.243	11	14.322	1.284
12	6.134	-0.251	12	14.327	1.285
13	6.129	-0.252	13	14.322	1.284
14	6.144	-0.249	14	14.337	1.287
15	6.144	-0.249	15	14.317	1.283
16	6.173	-0.243	16	14.322	1.284
17	6.212	-0.236	17	14.327	1.285
18	6.139	-0.250	18	14.332	1.286
19	8.341	+0.166	19	14.327	1.285
20	6.878	-0.110	20	14.317	1.283
21	6.305	-0.218	21	14.322	1.284
22	6.413	-0.198	22	14.317	1.283

FIGURE 45. SHADOWGRAPH PICTURE OF A GUIDE SURFACE PARACHUTE MODEL AT MACH NUMBER 1.072.

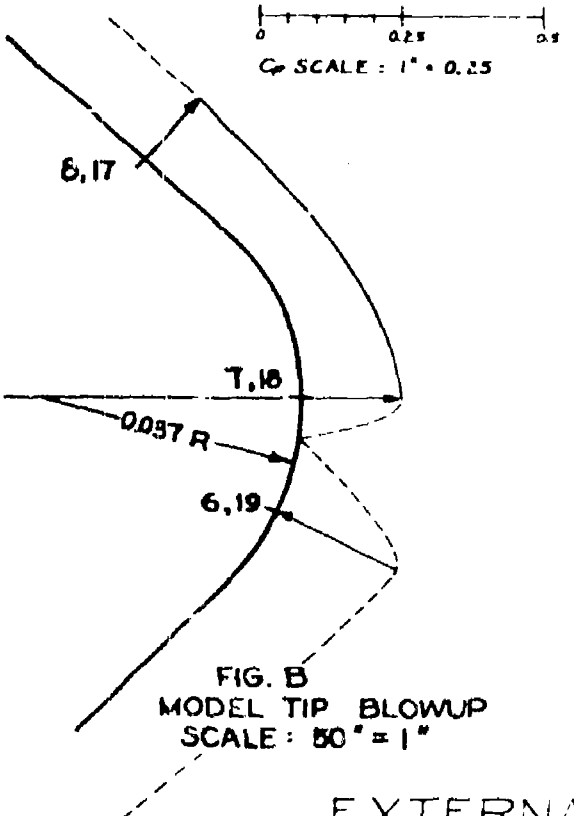

FIG. B
MODEL TIP BLOWUP
SCALE : 50" = 1"

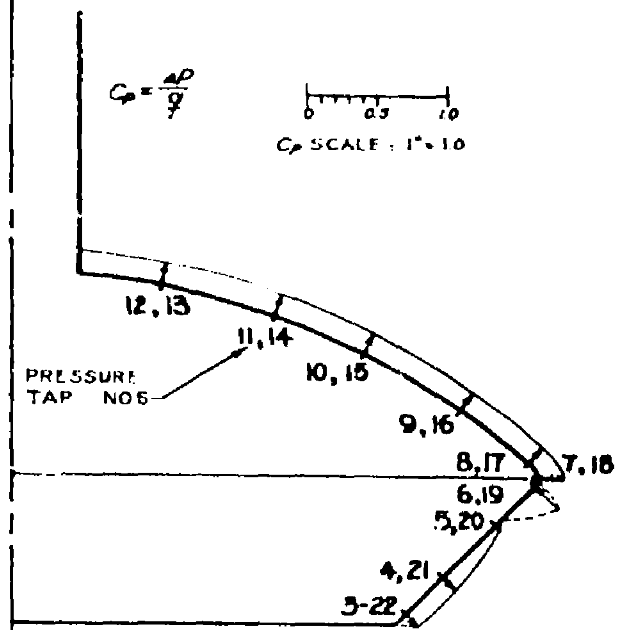

FIG. A
HALF MODEL
SCALE : 3" = 1"

EXTERNAL PRESSURE RUN
RUN NO. 6 C_p DISTRIBUTION ON
$2\frac{1}{2}$" GUIDE SURFACE PARACHUTE $M_\infty = 1.072$

FIG. 46

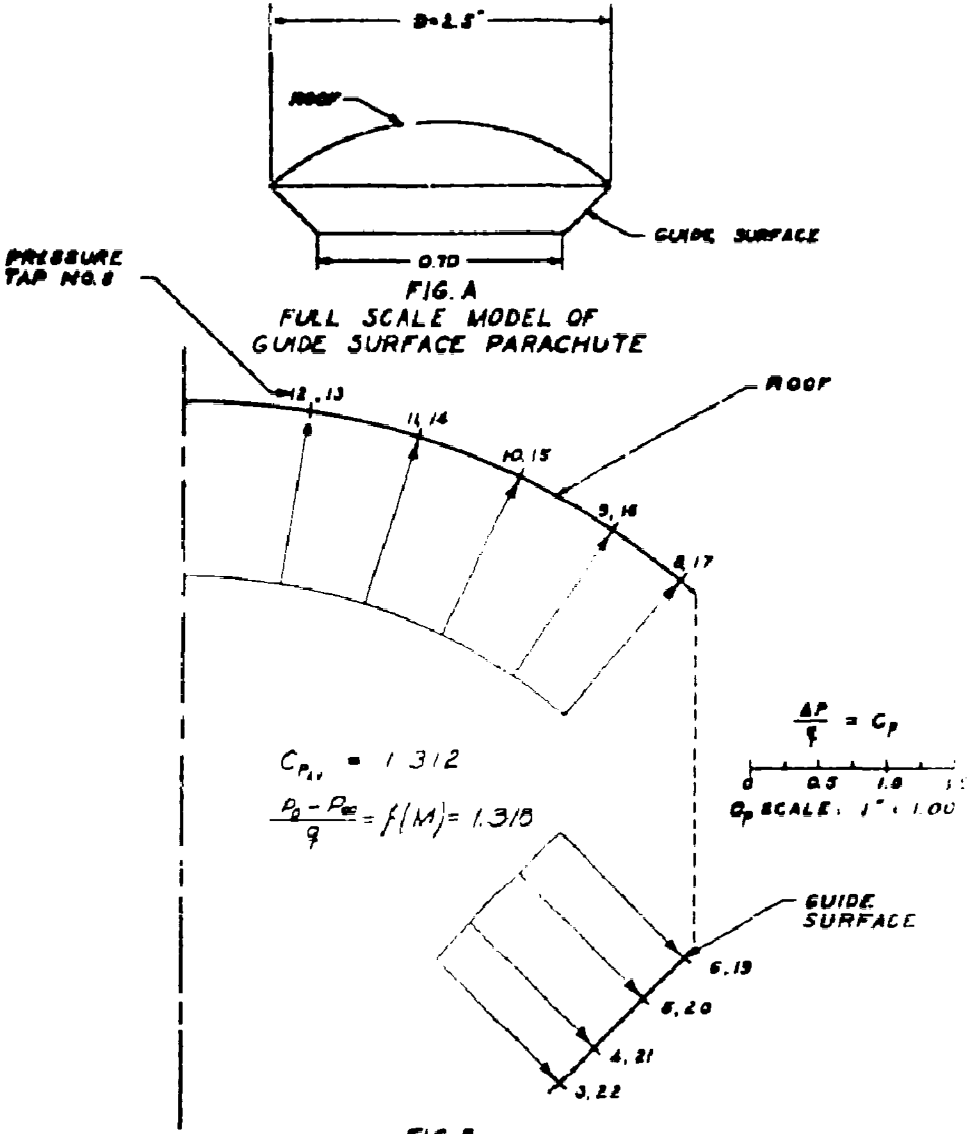

FIG. B
HALF MODEL. SURFACES DETACHED
SCALE: 3" = 1"

INTERNAL PRESSURE TEST
RUN NO. 14 C_p DISTRIBUTION ON
$2\frac{1}{2}$" GUIDE SURFACE PARACHUTE
$M_\infty = 1.067$
FIG 47

TABLE NO 14

GUIDE SURFACE PARACHUTE PRESSURE DISTRIBUTION

$M_{\infty_{AV}}$ = 1.07

EXTERNAL PRESSURE TEST M_∞ = 1.072 P_∞ = 6.902 psia, t = 78° F, P_0 = 14.237 psia, R_e = 9.59 × 10^5			INTERNAL PRESSURE TEST M_∞ ≐ 1.067 P_∞ = 6.987 psia, t = 94° F, P_0 = 14.324 psia, R_e = 9.09 × 10^5		
TAP NO.	P_L (psia)	C_p	TAP NO.	P_L (psia)	C_p (+)
3	6.235	−0.104	3	14.081	1.274
4	6.237	−0.120	4	14.291	1.312
5	6.702	−0.036	5	14.306	1.314
6	8.219	+0.237	6	14.301	1.314
7	5.841	−0.191	7	14.316	1.316
8	6.139	−0.137	8	14.306	1.314
9	6.071	−0.150	9	14.301	1.314
10	6.046	−0.154	10	14.306	1.314
11	6.046	−0.154	11	14.311	1.315
12	6.041	−0.155	12	14.311	1.315
13	6.041	−0.155	13	14.306	1.314
14	6.046	−0.154	14	14.306	1.314
15	6.041	−0.155	15	14.301	1.314
16	6.071	−0.150	16	14.301	1.314
17	6.115	−0.142	17	14.311	1.315
18	6.032	−0.157	18	14.311	1.315
19	8.165	+0.228	19	14.311	1.315
20	6.756	−0.026	20	14.301	1.314
21	6.227	−0.122	21	14.306	1.314
22	6.335	−0.102	22	14.301	1.314

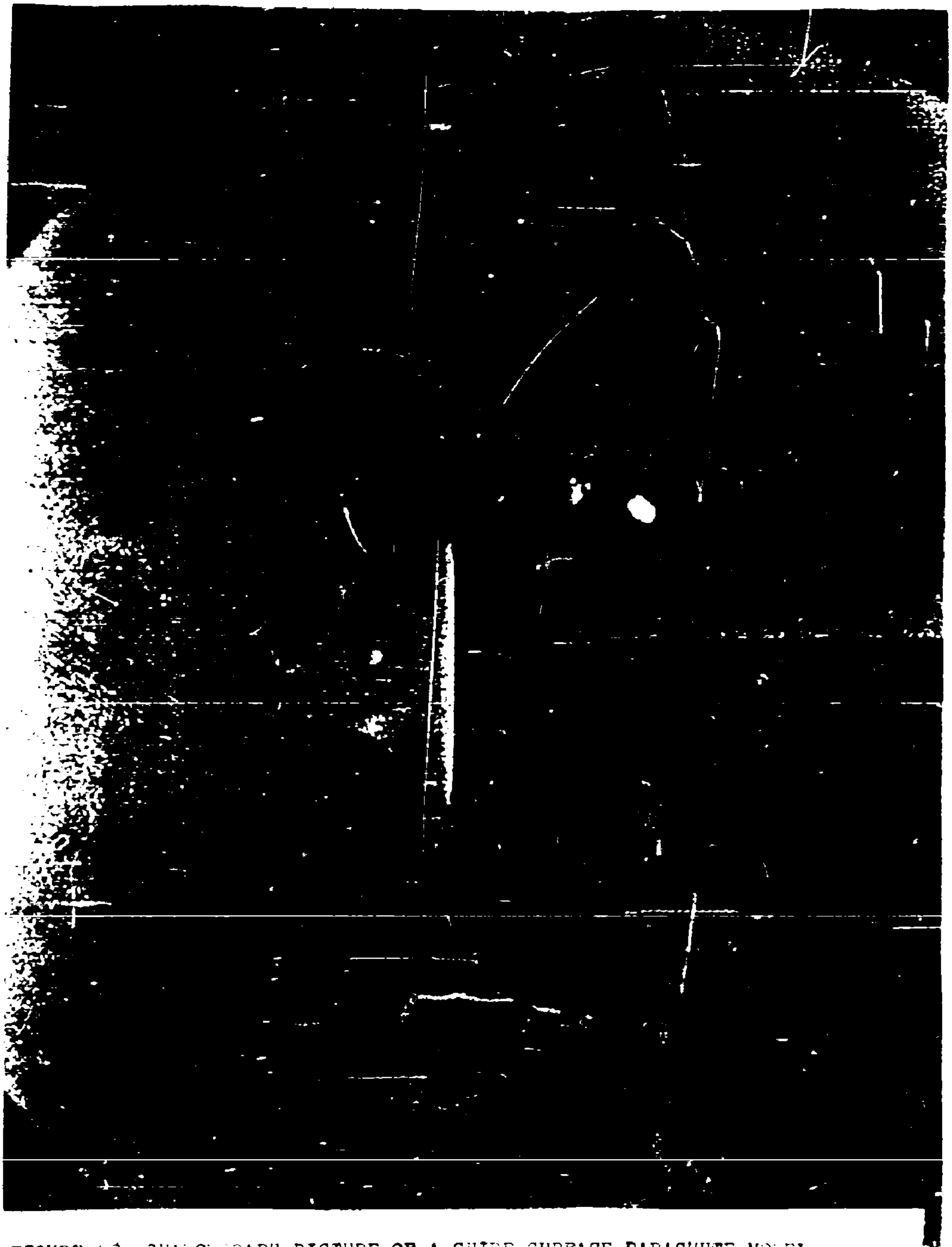

FIGURE 48. SHADOWGRAPH PICTURE OF A GUIDE SURFACE PARACHUTE MODEL AT MACH NUMBER 1.130.

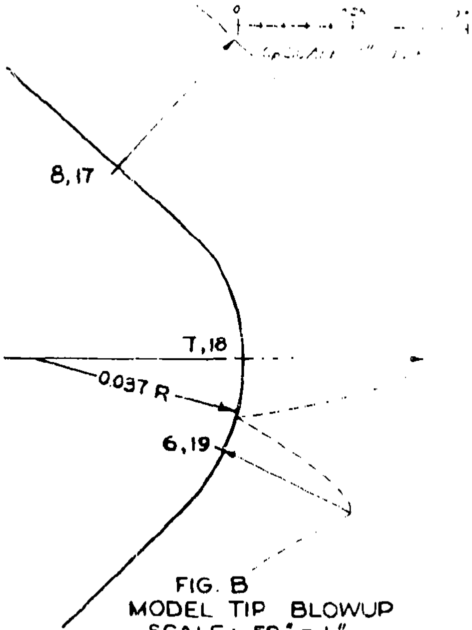

FIG. B
MODEL TIP BLOWUP
SCALE: 50" = 1"

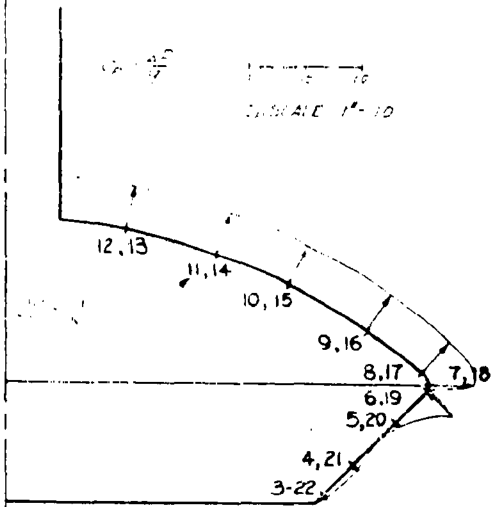

FIG. A
HALF MODEL
SCALE 3' = 1"

EXTERNAL PRESSURE RUN

RUN NO. 7 C_p DISTRIBUTION ON

$2\frac{1}{2}$" GUIDE SURFACE PARACHUTE $M_\infty = 1.130$

X

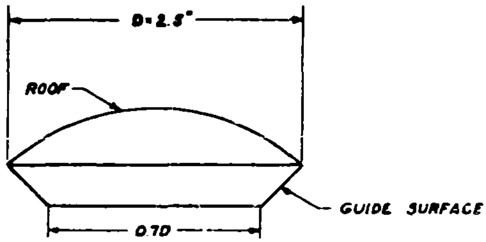

FIG. A
FULL SCALE MODEL OF
GUIDE SURFACE PARACHUTE

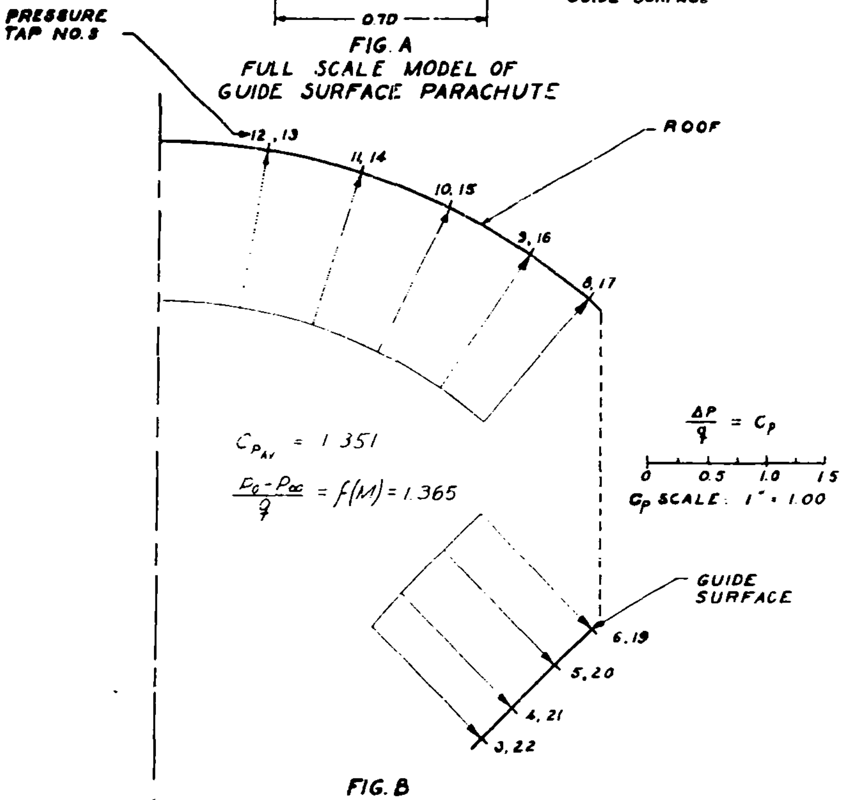

FIG. B
HALF MODEL : SURFACES DETACHED
SCALE : 3" = 1"

INTERNAL PRESSURE TEST
RUN NO. 5 C_p DISTRIBUTION ON
$2\frac{1}{2}$" GUIDE SURFACE PARACHUTE
$M_\infty = 1.135$
FIG. 50

TABLE NO. 1E

GUIDE SURFACE PARACHUTE PRESSURE DISTRIBUTION

$M_{\infty_{av}} = 1.13$

EXTERNAL PRESSURE TEST			INTERNAL PRESSURE TEST		
$M_\infty = 1.130$			$M_\infty = 1.135$		
$P_\infty = 6.424$ psia	$t = 72°$ F		$P_\infty = 6.422$ psia	$t = 90°$ F	
$P_0 = 14.241$ psia	$R_e = 9.65 \times 10^5$		$P_0 = 14.324$ psia	$R_e = 9.21 \times 10^5$	
TAP NO.	P_L (psia)	C_p	TAP NO.	P_L (psia)	C_p (+)
3	6.192	−0.040	3	14.017	1.312
4	6.109	−0.055	4	14.242	1.351
5	6.623	+0.035	5	14.257	1.353
6	8.174	+0.305	6	14.252	1.352
7	4.073	−0.410	7	14.267	1.355
8	4.445	−0.345	8	14.262	1.354
9	4.387	−0.355	9	14.252	1.352
10	4.338	−0.363	10	14.252	1.35[illegible]
11	4.352	−0.361	11	14.262	1.354
12	4.308	−0.368	12	14.262	1.354
13	4.191	−0.389	13	14.257	1.350
14	4.215	−0.385	14	14.257	1.350
15	4.215	−0.385	15	14.257	1.350
16	4.284	−0.373	16	14.262	1.354
17	4.338	−0.363	17	14.262	1.354
18	4.259	−0.377	18	14.267	1.355
19	8.179	+0.306	19	14.262	1.354
20	6.735	+0.054	20	14.257	1.350
21	6.124	−0.052	21	14.257	1.350
22	6.246	−0.031	22	14.252	1.352

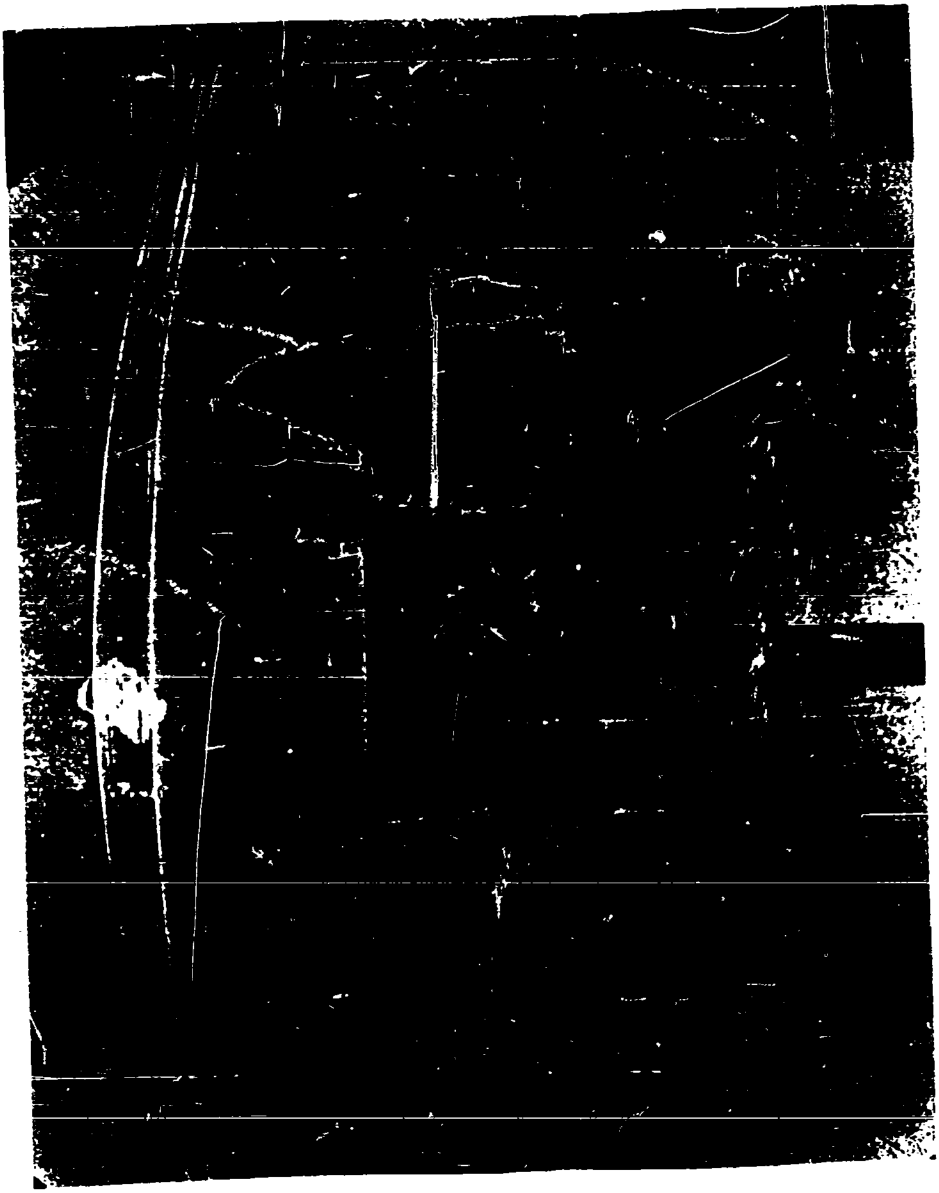

FIGURE 51. SHADOWGRAPH PICTURE OF A GUIDE SURFACE PARACHUTE MODEL AT MACH NUMBER 1.234.

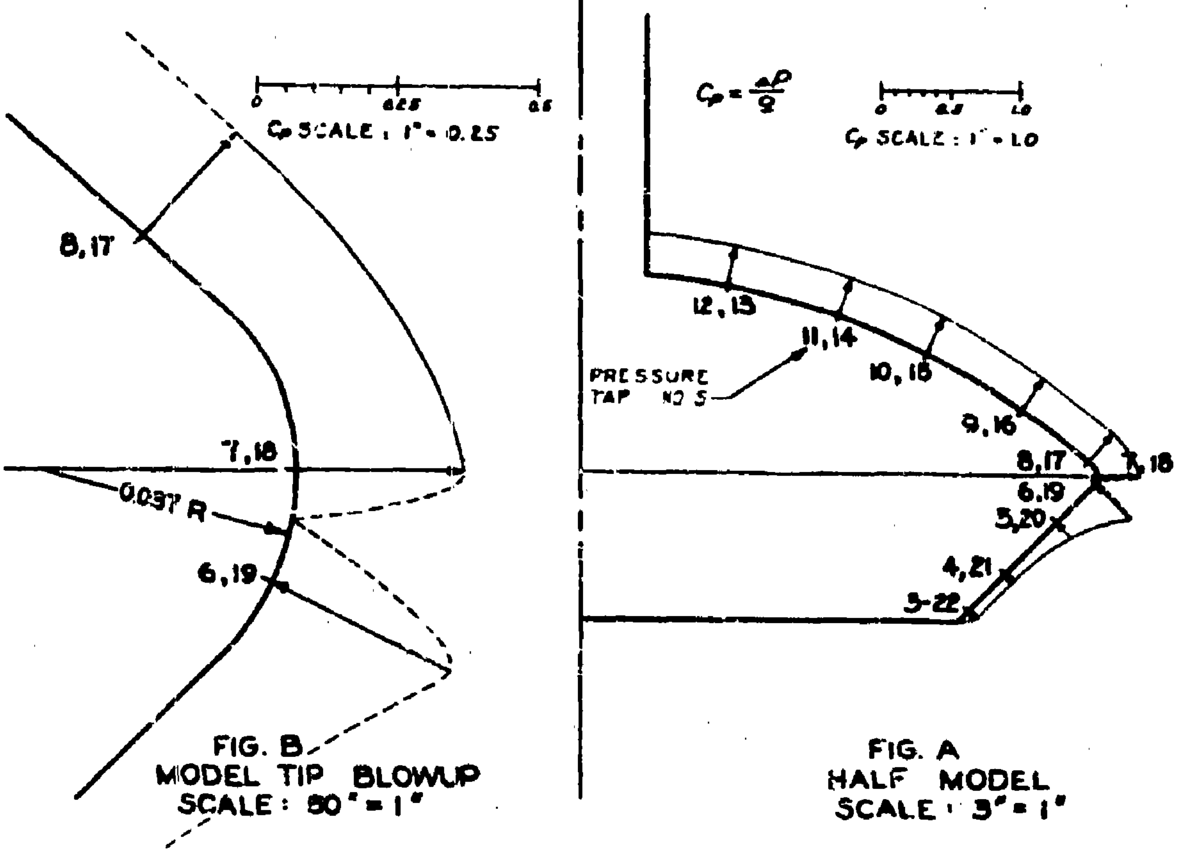

EXTERNAL PRESSURE RUN
RUN NO. 6 C_p DISTRIBUTION ON
$2\frac{1}{2}$" GUIDE SURFACE PARACHUTE $M_\infty = 1.234$

FIG. 52

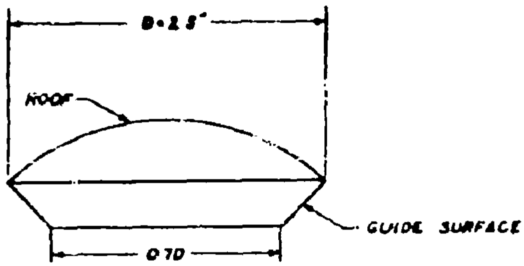

FIG. A
FULL SCALE MODEL OF
GUIDE SURFACE PARACHUTE

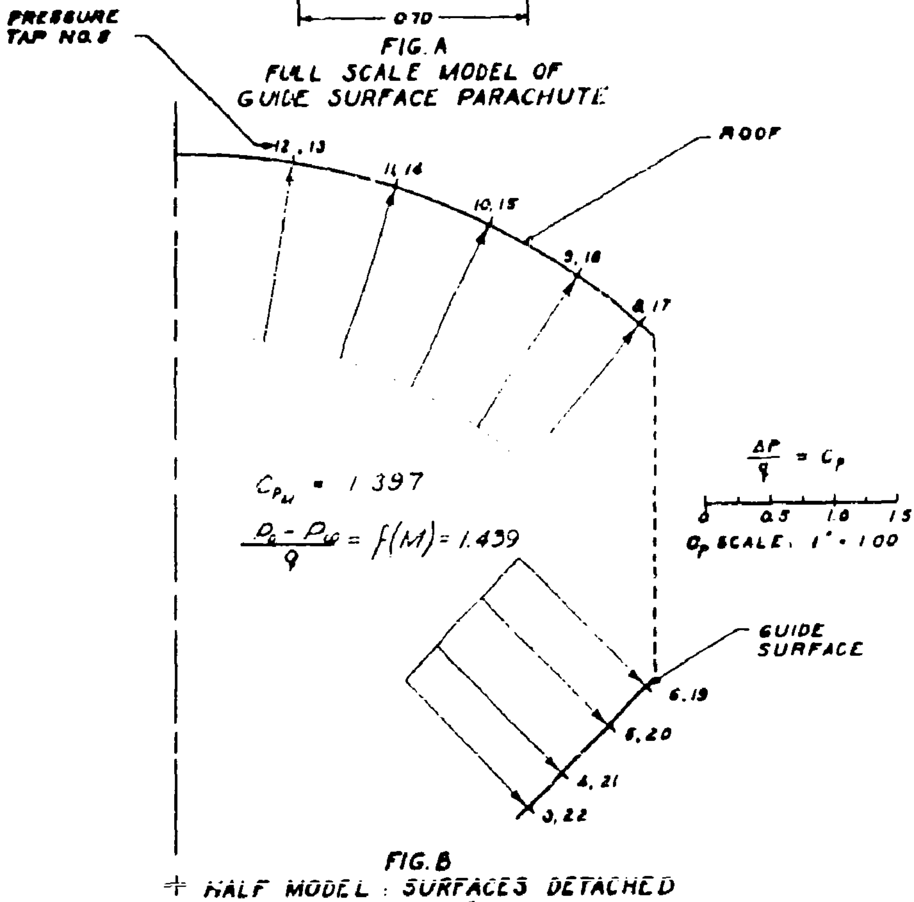

FIG. B
HALF MODEL : SURFACES DETACHED
SCALE : 3" = 1"

INTERNAL PRESSURE TEST
RUN NO. 16 C_p DISTRIBUTION ON
$2\frac{1}{2}$" GUIDE SURFACE PARACHUTE
M_∞ = 1.230
FIG 53

TABLE NO. 16

GUIDE SURFACE PARACHUTE PRESSURE DISTRIBUTION

$M_{\infty_{av}}$ = 1.23

EXTERNAL PRESSURE TEST $M_\infty = 1.234$ P_∞ = 5.615 psia, t = 72° F, P_0 = 14.241 psia, $R_e = 9.71 \times 10^5$			INTERNAL PRESSURE TEST $M_\infty = 1.230$ P_∞ = 5.678 psia, t = 90° F, P_0 = 14.324 psia, $R_e = 9.28 \times 10^5$		
TAP NO.	P_L (psia)	C_p	TAP NO	P_L (psia)	C_p (+)
3	6.126	+ 0.342	3	13.880	1.364
4	6.043	+ 0.286	4	14.086	1.398
5	6.508	+ 0.596	5	14.091	1.399
6	7.839	+ 1.486	6	14.091	1.399
7	3.724	-1.264	7	14.091	1.399
8	4.149	- 0.980	8	14.091	1.399
9	4.081	-1.026	9	14.081	1.397
10	4.012	-1.071	10	14.086	1.398
11	4.032	1.058	11	14.096	1.400
12	3.963	-1.104	12	14.081	1.397
13	3.880	-1.160	13	14.086	1.398
14	3.919	-1.133	14	14.091	1.399
15	3.929	-1.127	15	14.091	1.399
16	3.993	-1.084	16	14.086	1.398
17	4.056	-1.042	17	14.086	1.398
18	3.968	-1.101	18	14.096	1.400
19	7.614	+1.336	19	14.091	1.399
20	6.380	+0.512	20	14.086	1.398
21	5.935	+0.214	21	14.086	1.398
22	6.018	+0.270	22	14.081	1.397

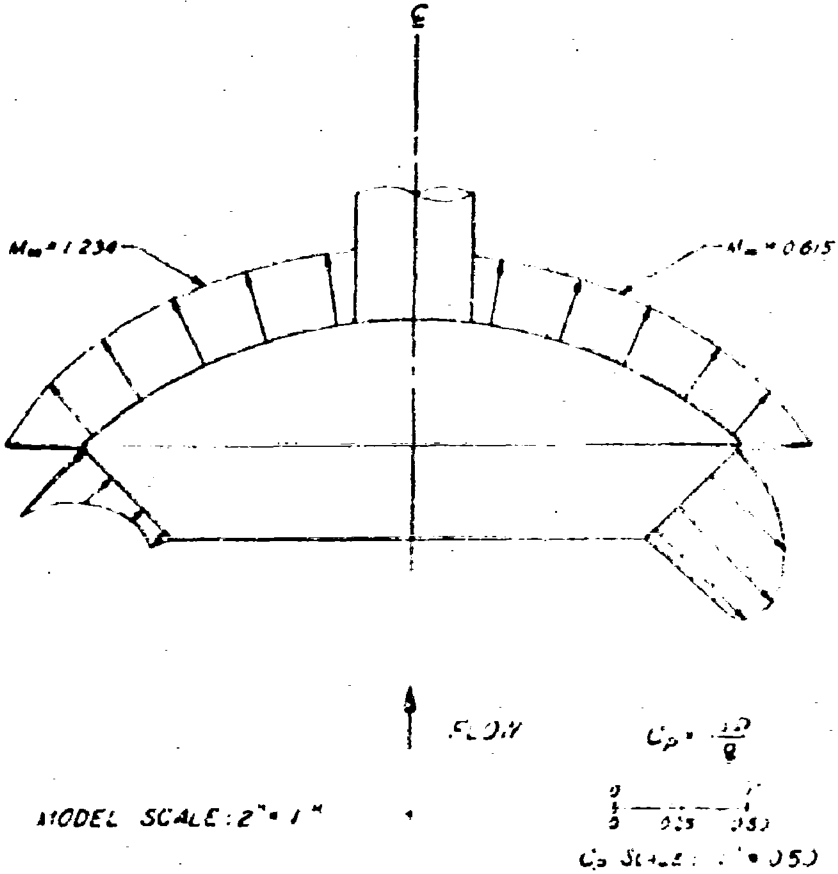

RANGE OF C_p FOR EXTERNAL PRESSURE TEST ON A $2\frac{1}{2}$ IN. DIA. GUIDE SURFACE PARACHUTE MODEL
AVERAGE VALUES OF C_p PLOTTED ON HALF MODELS

FIG. 54

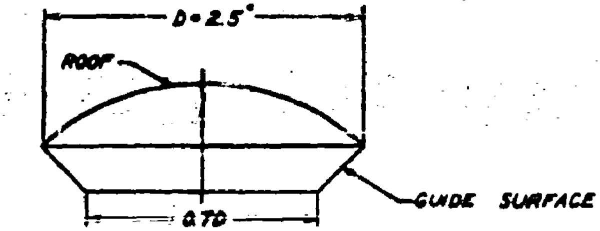

FIG. A
FULL SCALE MODEL OF
GUIDE SURFACE PARACHUTE

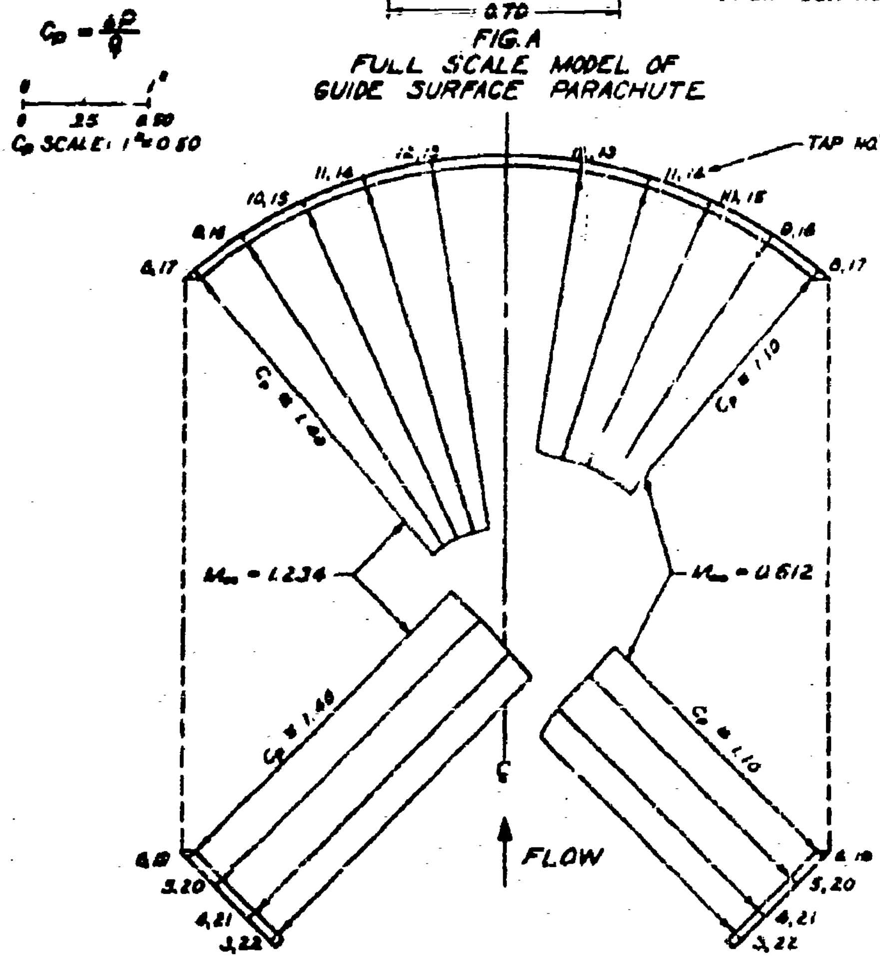

FIG. B
SURFACES DETACHED
SCALE: 2" = 1"

RANGE OF C_p FOR INTERNAL PRESSURE TEST
ON A $2\frac{1}{2}$ IN. DIA GUIDE SURFACE PARACHUTE MODEL
AVERAGE VALUES OF C_p PLOTTED ON HALF MODELS

EXTERNAL PRESSURE DISTRIBUTION vs FLATTENED SURFACE FOR VARIOUS M_∞

MODEL: $2\frac{1}{2}$ INCH DIAMETER GUIDE SURFACE PARACHUTE

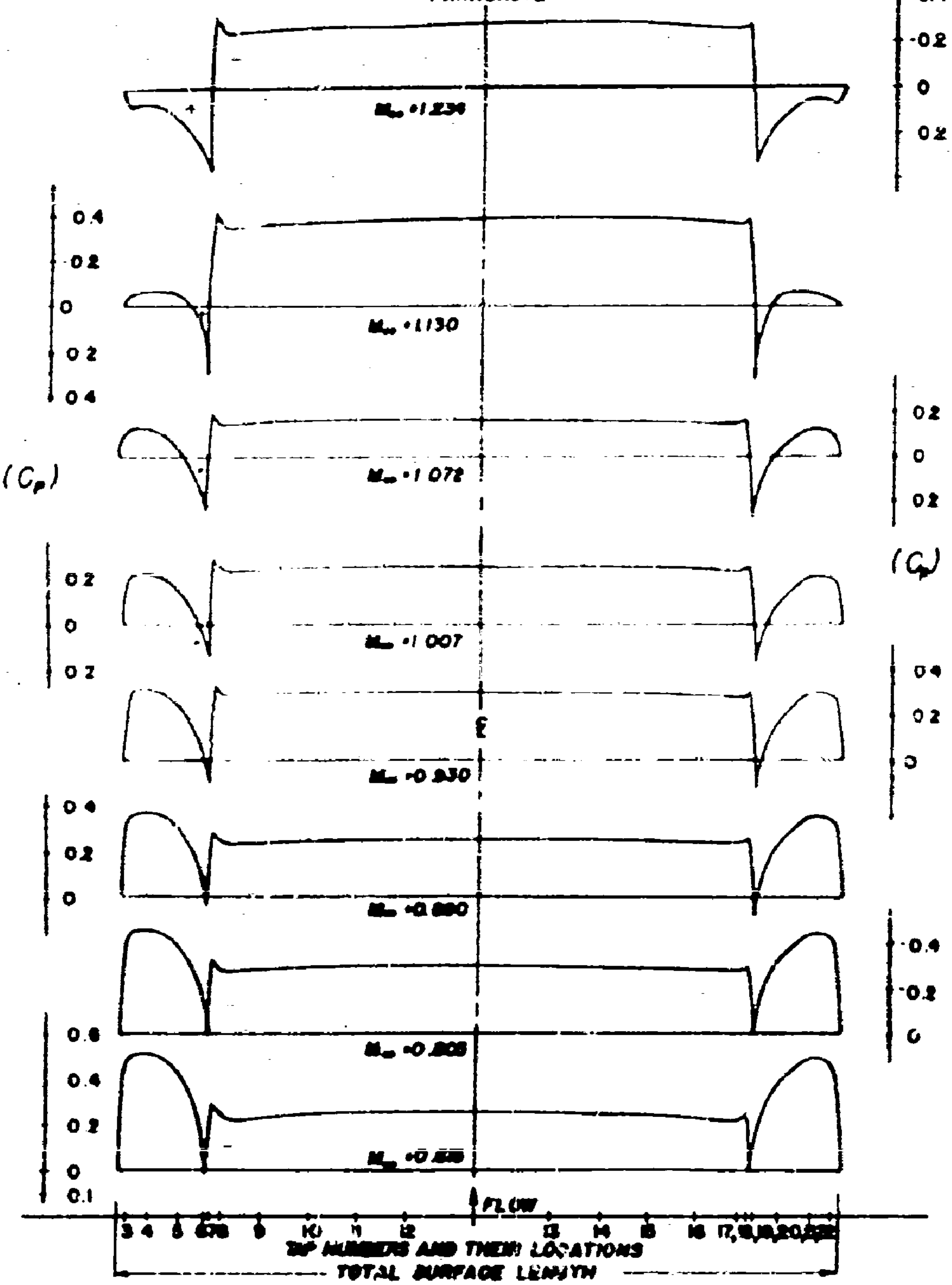

FIG 56

AVERAGE EXTERNAL PRESSURE COEFFICIENT (C_p) VS MACH NUMBER (M_{∞})
FOR PARACHUTE PRESSURE TAPS
MODEL : 2.5 IN DIA RIBBON PARACHUTE
FIG 87

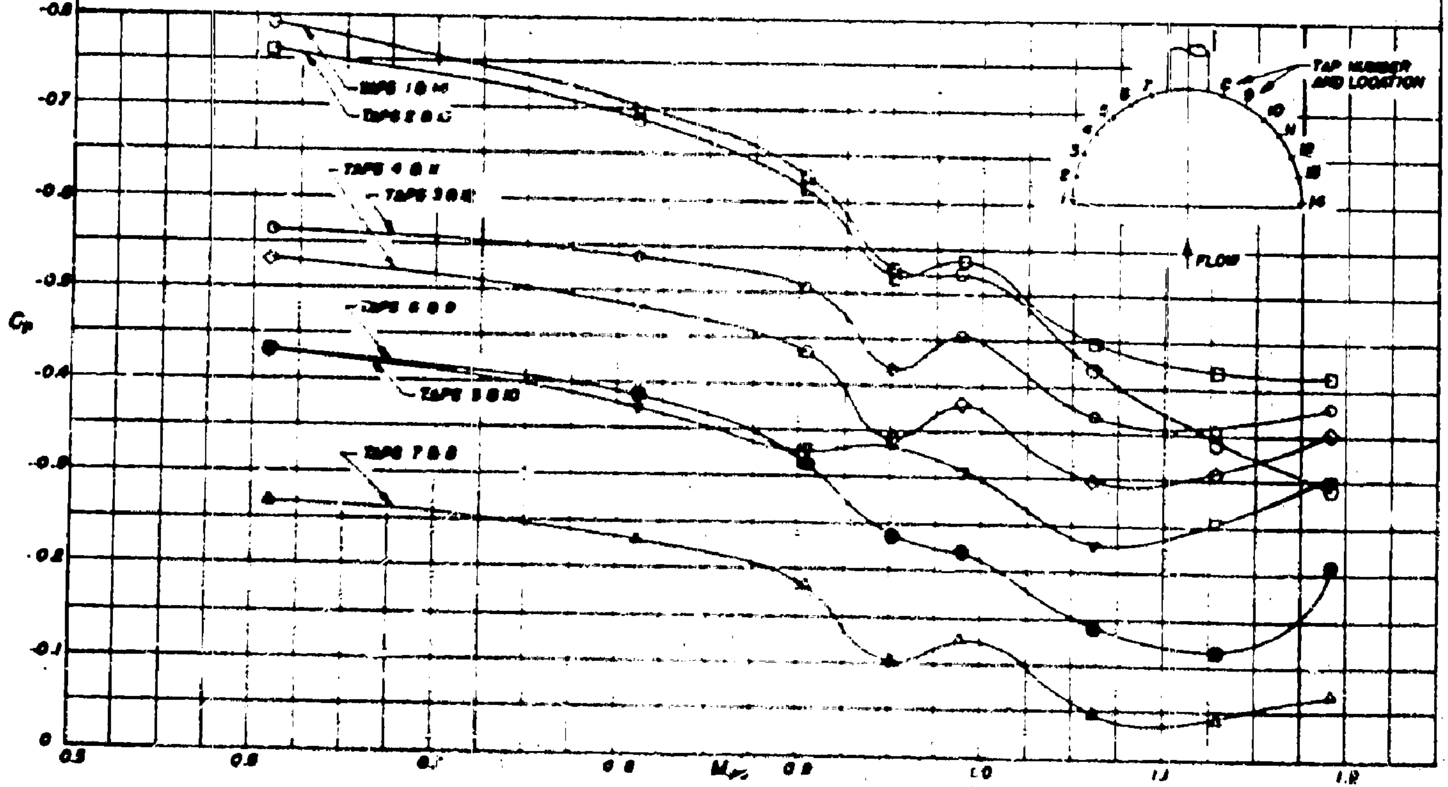

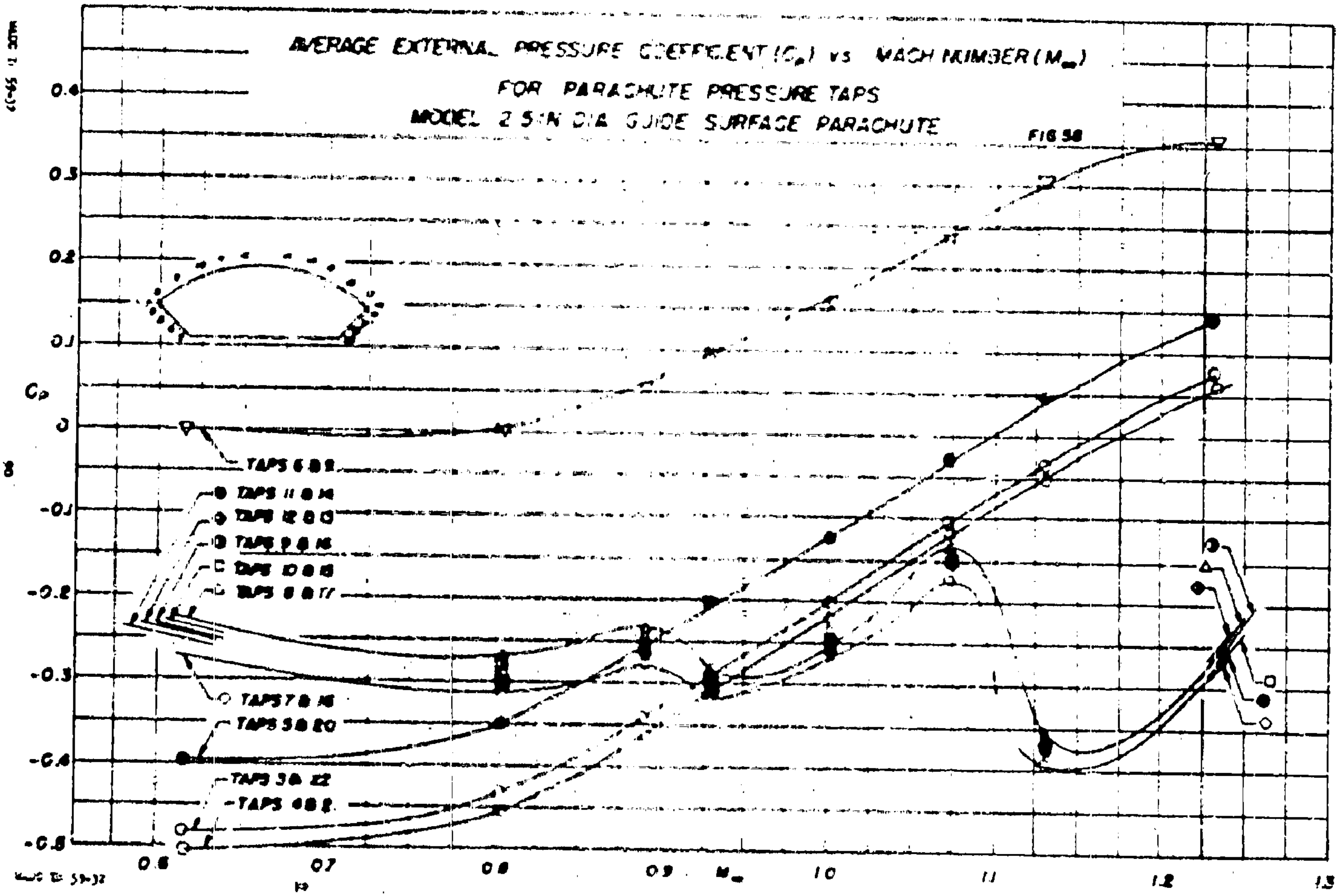
AVERAGE EXTERNAL PRESSURE COEFFICIENT (C_p) vs MACH NUMBER (M_∞)
FOR PARACHUTE PRESSURE TAPS
MODEL 2.5 IN DIA GUIDE SURFACE PARACHUTE
FIG 58
C_p
M_∞
TAPS 6 & 2
TAPS 11 & 14
TAPS 12 & 13
TAPS 9 & 16
TAPS 10 & 15
TAPS 8 & 17
TAPS 7 & 18
TAPS 5 & 20
TAPS 3 & 22
TAPS 4 & 2
0.4
0.3
0.2
0.1
0
-0.1
-0.2
-0.3
-0.4
-0.5
0.6
0.7
0.8
0.9
1.0
1.1
1.2
1.3

UNCLASSIFIED

AD 210257

Armed Services Technical Information Agency

ARLINGTON HALL STATION
ARLINGTON 12 VIRGINIA

FOR
MICRO CARD
CONTROL ONLY

3 OF 3

UNCLASSIFIED